Zoologischer Anzeiger 286 (2020) 117–134

Contents lists available at ScienceDirect

Zoologischer Anzeiger

journal homepage: www.elsevier.com/locate/jcz

Research paper

An integrative description of *Minibiotus ioculator* sp. nov. from the Republic of South Africa with notes on *Minibiotus pentannulatus* Londoño et al., 2017 (Tardigrada: Macrobiotidae)

Daniel Stec [a, *], Reinhardt Møbjerg Kristensen [b], Łukasz Michalczyk [a]

[a] Institute of Zoology and Biomedical Research, Jagiellonian University, Gronostajowa 9, 30-387 Kraków, Poland
[b] Section of Biosystematics, Zoological Museum, Natural History Museum of Denmark, University of Copenhagenø, Universitetsparken 15, DK-2100, Copenhagen, Denmark

ARTICLE INFO

Article history:
Received 12 February 2020
Received in revised form
25 March 2020
Accepted 25 March 2020
Available online 6 April 2020

Corresponding Editor: P. Michalik

Keywords:
Africa
Biodiversity
DNA barcodes
New species
Peribuccal structures
Taxonomy

ABSTRACT

The genus *Minibiotus* is morphologically diverse, which may suggest its polyphyletic character. However, scarce genetic data and often also the lack of detailed morphological data currently do not allow for the verification of the relationships within this genus. Here, for the very first time, we provide an integrative description of a new *Minibiotus* species. *Minibiotus ioculator* **sp. nov.** from the Republic of South Africa differs from other congeners mainly by egg ornamentation with processes on the egg shell that resemble the hat of a royal jester. We also provide new taxonomic data on *Minibiotus pentannulatus* based on a population newly found in Tanzania, which constitutes the first African record of this species originally described from South America. Our study involved both classical taxonomic methods, which include morphological and morphometric analyses conducted with the use of light and scanning electron microscopy, and genetic data in the form of DNA sequences of four markers (three nuclear: 18S rRNA, 28S rRNA, ITS-2, and one mitochondrial: COI). The results of this study allow a discussion of species composition within *Minibiotus* and question the validity of the current diagnosis of the genus.

1. Introduction

Tardigrada are a phylum of microscopic invertebrates known also as water bears. Tardigrades are distributed globally and they inhabit various environments, from ocean depths to mountain peaks, and from polar caps to tropical forests (Nelson et al. 2015). Up to date, about 1300 species have been described in the phylum (Guidetti & Bertolani 2005; Degma & Guidetti 2007; Degma et al. 2009–2019).

The genus *Minibiotus* R.O. Schuster, 1980 was erected fourty years ago by Schuster et al. (1980). Almost two decades later Claxton (1998) published a comprehensive revision of this cosmopolitan genus, which then encompassed 22 species and currently comprises 48 species (Degma et al. 2009–2019). However, only nine *Minibiotus* species have been reported from Africa so far, out of which five were described specifically from this continent. These are: *Minibiotus africanus* Binda & Pilato, 1995, *Minibiotus allani* (Murray, 1913), *Minibiotus crassidens* (Murray, 1907), *Minibiotus granatai* (Pardi, 1941), and *Minibiotus harrylewisi* Meyer & Hinton, 2009.

Currently, genetic data for the genus are very scarce. Specifically, there are only fourteen *Minibiotus* DNA sequences deposited in GenBank. Moreover, almost all of them are unidentified species or the entries are identified as "*Minibiotus intermedius* (Plate, 1888)" of which a certain identification is impossible due to the outdated and incomplete original description. In fact, there is only one named species, *Minibiotus gumersindoi* Guil & Guidetti, 2005, which is associated with multiple (i.e. 18S rRNA, 28S rRNA and COI) sequences (Guil & Giribet 2012). The currently available DNA sequences suggest that *Minibiotus* is most likely polyphyletic and some species are closely related to *Paramacrobiotus* Guidetti et al., 2009, forming together one of the two major evolutionary lineages within Macrobiotidae (Bertolani et al. 2014). However, the extremely limited genetic data prevent any sound conclusions on the phylogenetic character and position of the genus *Minibiotus*. The putative polyphyly of *Minibiotus* is also suggested by the morphological heterogeneity of the genus, which comprises

* Corresponding author.
E-mail address: daniel_stec@interia.eu (D. Stec).

https://doi.org/10.1016/j.jcz.2020.03.007

Table 1
PCR primers for amplification of the four DNA fragments sequenced in the study.

DNA fragment	Primer name	Primer direction	Primer sequence (5′-3′)	Primer source
18S rRNA	18S_Tar_1Ff	forward	AGGCGAAACCGCGAATGGCTC	Stec et al. (2017)
	18S_Tar_1Rr	reverse	GCCGCAGGCTCCACTCCTGG	
28S rRNA	28S_Eutar_F	forward	ACCCGCTGAACTTAAGCATAT	Gąsiorek et al. (2018), Mironov et al. (2012)
	28SR0990	reverse	CCTTGGTCCGTGTTTCAAGAC	
ITS-2	Eutar_Ff	forward	CGTAACGTGAATTGCAGGAC	Stec et al. (2018b)
	Eutar_Rr	reverse	TCCTCCGCTTATTGATATGC	
COI	LCO1490	forward	GGTCAACAAATCATAAAGATATTGG	Folmer et al. (1994)
	HCO2198	reverse	TAAACTTCAGGGTGACCAAAAAATCA	
	HCOoutout	reverse	GTAAATATATGRTGDGCTC	Prendini et al. (2005)

species with two and three macroplacoids in the pharynx, species with and without pores in the body cuticle, or species with egg processes enclosed within membrane and with naked processes (Stec et al. 2015). The broad morphological diagnosis combined with the small size of specimens which entails difficulties in the determination of some characters (e.g. peribuccal structures) sometimes result in erroneous assignments of species to the genus (e.g. see Stec et al. 2015 who transferred two *Minibiotus* species to the genus *Macrobiotus*).

In this paper, we provide the first description of a new *Minibiotus* species by means of integrative taxonomy. In addition to the description of *Minibiotus ioculator* **sp. nov.** from the Republic of South Africa, we also present integrative data and amend the description of *Minibiotus pentannulatus* Londoño, Daza, Lisi & Quiroga, 2017 based on a newly found population from Tanzania. The detailed morphological and morphometric data were obtained using light contrast and scanning electron microscopy. These data are associated with DNA sequences of four genetic markers standardly used in tardigrade taxonomy (the nuclear 18S rRNA, 28S rRNA, and ITS-2, and the mitochondrial *COI*).

2. Material and methods

2.1. Samples collection and processing

The lichen sample containing the new species was collected by Witold Morek and Bartłomiej Surmacz on 7 September 2018 from the rock in forest in the Tradouw Pass located in Western Cape, South Africa (33°58′58.44″S, 20°42′17.88″E; 295 m asl). The lichen sample containing *M. pentannulatus* was collected by Thomas Pape on 16 August 2016 from branches of a bush, near the Mwanihana Peak in the Udzungwa Mts. National Park in Tanzania (7°49′25″S, 36°49′32″E; 2050 m asl). The latter sample contained also a new species of the *Macrobiotus hufelandi* group, which has been recently described as *Macrobiotus papei* Stec, Kristensen & Michalczyk, 2018a.

The samples were examined for tardigrades using the protocol by Dastych (1980) with modifications described in detail in Stec et al. (2015). A total of 99 and 83 animals and 31 and 46 eggs of the two *Minibiotus* species were extracted from the South African and Tanzanian samples, respectively. In order to perform integrative taxonomic descriptions, the isolated animals and eggs were split into three groups for specific analyses: morphological analysis with phase and differential contrast light microscopy, morphological analysis with scanning electron microscopy, and DNA sequencing (for details see sections “Material examined” provided below for each description).

2.2. Microscopy and imaging

Specimens for light microscopy were mounted on microscope slides in a small drop of Hoyer's medium and secured with a cover slip, following the protocol by Morek et al. (2016). Slides were examined under an Olympus BX53 light microscope with phase and Nomarski contrast (PCM and NCM, respectively), collectively termed as light contrast microscopy (LCM), associated with an Olympus DP74 digital camera. Immediately after mounting, the specimens in the medium slides where also checked under PCM for the presence of males and females in the studied population as the spermatozoa in testis and spermathecae are visible for several hours after mounting (Coughlan et al. 2019; Coughlan & Stec 2019). In order to obtain clean and extended specimens for SEM, tardigrades were processed according to the protocol by Stec et al. (2015). Bucco-pharyngeal apparatuses were extracted following the protocol of Eibye-Jacobsen (2001) as modified by Gąsiorek et al. (2016). Specimens were examined under high vacuum in a *Versa 3D DualBeam* Scanning Electron Microscope (SEM) at the ATOMIN facility of the Jagiellonian University, Kraków, Poland. All figures were

Table 2
GenBank accession numbers sequences of the *Minibiotus* species analysed in this study. Bolded numbers indicate newly obtained sequences whereas underlined numbers indicate type sequences.

DNA marker	Species	Accession number	Source
18S rRNA	*M. ioculator* **sp. nov.**	**MT023998**	**This study**
	M. pentannulatus Londoño et al., 2017	**MT023999**	**This study**
	M. gumersindoi Guil & Guidetti, 2005	FJ435748	Guil & Giribet (2012)
	M. intermedius group	HQ604979–80	Bertolani et al. (2014)
	Minibiotus sp.	EU266932–4	Sands et al. (2008)
28S rRNA	*M. ioculator* **sp. nov.**	**MT024041**	**This study**
	M. pentannulatus Londoño et al., 2017	**MT024042 –3**	**This study**
	M. gumersindoi Guil & Guidetti, 2005	FJ435761	Guil & Giribet (2012)
ITS-2	*M. ioculator* **sp. nov.**	**MT024000**	**This study**
	M. pentannulatus Londoño et al., 2017	**MT024001**	**This study**
COI	*M. ioculator* **sp. nov.**	**MT023412**	**This study**
	M. pentannulatus Londoño et al., 2017	**MT023413–4**	**This study**
	M. gumersindoi Guil & Guidetti, 2005	FJ435803	Guil & Giribet (2012)

Table 3
Measurements [in μm] of selected morphological structures of individuals of *Minibiotus ioculator* **sp. nov.** mounted in Hoyer's medium (N–number of specimens/structures measured, RANGE refers to the smallest and the largest structure among all measured specimens; SD–standard deviation).

CHARACTER	N	RANGE		MEAN		SD		Holotype	
		μm	*pt*	μm	*pt*	μm	*pt*	μm	*pt*
Body length	30	197–371	*891–1267*	313	*1121*	43	*85*	312	*1106*
Buccopharyngeal tube									
Buccal tube length	30	21.8–30.8	–	27.8	–	2.3	–	28.2	–
Stylet support insertion point	30	13.4–19.1	*61.1–62.8*	17.3	*62.2*	1.5	*0.5*	17.7	*62.8*
Buccal tube external width	30	1.8–2.4	*6.4–8.6*	2.1	*7.7*	0.2	*0.5*	2.1	*7.4*
Buccal tube internal width	30	0.7–1.6	*2.8–6.0*	1.0	*3.8*	0.2	*0.6*	0.8	*2.8*
Ventral lamina length	30	9.3–13.9	*41.9–49.5*	12.4	*44.6*	1.1	*1.8*	12.5	*44.3*
Placoid lengths									
Macroplacoid 1	30	2.0–3.4	*8.9–12.4*	2.9	*10.5*	0.3	*0.8*	3.0	*10.6*
Macroplacoid 2	30	1.5–2.4	*6.4–8.4*	2.0	*7.3*	0.2	*0.5*	2.2	*7.8*
Macroplacoid 3	30	1.8–3.0	*7.8–10.2*	2.5	*8.9*	0.2	*0.6*	2.3	*8.2*
Microplacoid	30	0.7–1.6	*2.9–5.3*	1.1	*3.9*	0.2	*0.6*	1.0	*3.5*
Macroplacoid row	30	6.3–10.4	*27.0–35.3*	8.8	*31.6*	0.9	*1.7*	8.9	*31.6*
Placoid row	30	7.2–12.4	*32.1–41.4*	10.2	*36.8*	1.1	*2.1*	10.4	*36.9*
Claw 1 heights									
External primary branch	28	5.1–8.2	*23.2–29.0*	7.2	*26.2*	0.8	*1.4*	7.7	*27.3*
External secondary branch	27	3.7–6.7	*16.9–24.0*	5.6	*20.4*	0.7	*1.7*	6.0	*21.3*
Internal primary branch	29	4.9–7.9	*22.1–29.0*	6.9	*24.8*	0.7	*1.4*	7.0	*24.8*
Internal secondary branch	28	3.5–6.4	*15.4–23.7*	5.4	*19.3*	0.7	*1.6*	5.6	*19.9*
Claw 2 heights									
External primary branch	27	5.3–9.1	*23.9–31.3*	7.9	*28.3*	0.7	*1.5*	8.2	*29.1*
External secondary branch	24	3.7–7.1	*16.7–25.2*	6.3	*22.7*	0.8	*1.6*	6.7	*23.8*
Internal primary branch	27	5.1–8.4	*23.0–30.5*	7.5	*26.8*	0.7	*1.6*	7.6	*27.0*
Internal secondary branch	26	3.6–6.9	*16.2–24.0*	5.9	*21.0*	0.7	*1.8*	6.0	*21.3*
Claw 3 heights									
External primary branch	28	5.3–9.3	*23.9–32.4*	7.9	*28.6*	0.9	*1.8*	8.3	*29.4*
External secondary branch	22	3.7–7.2	*16.7–26.3*	6.2	*22.5*	0.9	*2.0*	6.7	*23.8*
Internal primary branch	28	5.1–8.4	*23.0–28.4*	7.4	*26.8*	0.8	*1.5*	7.8	*27.7*
Internal secondary branch	23	3.6–6.8	*16.2–23.6*	5.8	*21.1*	0.8	*1.9*	6.2	*22.0*
Claw 4 heights									
Anterior primary branch	27	6.2–10.2	*27.9–35.9*	8.9	*31.9*	0.9	*1.8*	8.5	*30.1*
Anterior secondary branch	24	5.1–8.2	*20.6–26.6*	6.8	*24.1*	0.6	*1.4*	6.2	*22.0*
Posterior primary branch	26	7.2–11.2	*30.7–40.5*	9.7	*35.0*	1.0	*2.2*	9.8	*34.8*
Posterior secondary branch	18	5.4–8.1	*23.9–28.1*	7.2	*25.8*	0.7	*1.2*	7.4	*26.2*

pt values in tardigrade measurements are always provided with italics.

assembled in Corel Photo-Paint X6, ver. 16.4.1.1281. For structures that could not be satisfactorily focused in a single light microscope photograph, a stack of 2–6 images were taken with an equidistance of ca. 0.2 μm and assembled manually into a single deep-focus image in Corel Photo-Paint X6, ver. 16.4.1.1281.

2.3. Morphometrics and morphological nomenclature

All measurements are given in micrometres (μm). Sample size was adjusted following recommendations by Stec et al. (2016). Structures were measured only if their orientation was suitable. Body length was measured from the anterior extremity to the end of the body, excluding the hind legs. The terminology used to describe oral cavity armature and egg shell morphology follows Michalczyk & Kaczmarek (2003) and Kaczmarek & Michalczyk (2017). The type of buccal apparatus and claws are given according to Pilato & Binda (2010). Macroplacoid length sequence is given according to Kaczmarek et al. (2014). Buccal tube length and the level of the stylet support insertion point were measured according to Pilato (1981). The *pt* index is the ratio of the length of a given structure to the length of the buccal tube expressed as a percentage (Pilato 1981). All other measurements and nomenclature follow Kaczmarek & Michalczyk (2017). Morphometric data were handled using the "Parachela" ver. 1.7 template available from the Tardigrada Register (Michalczyk & Kaczmarek 2013). Raw morphometric data for each analysed species are provided as supplementary materials (SM.01 and SM.02). Data underlying the description of the new species are also deposited in Tardigrada Register under www.tardigrada.net/register/0063.htm. Tardigrade taxonomy follows Guil et al. (2019).

2.4. Comparative material

To identify the Tanzanian population, beside the original description by Londoño et al. (2017), we also used microphotographs of a *M. pentannulatus* paratype kindly sent to us by Rosana Londoño and Anisbeth Daza (Universidad del Magdalena, Colombia).

2.5. Genotyping

Individual DNA extractions were made from animals and/or eggs following a modified protocol by Casquet et al. (2012). Each specimen was placed individually in a 1.5 ml Eppendorf micro-centrifuge tube, in 45 μl of a 3% suspension of 75–150 μm wet bead size Chelex® 100 resin (Bio-Rad) in ddH2O with addition of 3.0 μl Proteinase K (A&A Biotechnology) and incubated at 56 °C for

Table 4
Measurements [in μm] of selected morphological structures of the eggs of *Minibiotus ioculator* **sp. nov.** mounted in Hoyer's medium (N–number of eggs/structures measured, RANGE refers to the smallest and the largest structure among all measured specimens; SD–standard deviation).

CHARACTER	N	RANGE	MEAN	SD
Egg full diameter	14	66.2–81.1	73.6	4.3
Egg bare diameter	14	54.2–70.1	61.9	4.1
Process height	42	4.5–7.9	5.6	0.9
Process base width	42	2.1–4.2	2.9	0.4
Process base/height ratio	42	41%–69%	53%	7%
Inter-process distance	42	1.2–3.0	2.1	0.4
Number of processes on the egg circumference	14	30–32	31.3	0.8

Table 5
Measurements [in μm] of selected morphological structures of individuals of *Minibiotus pentannulatus* Londoño, Daza, Lisi & Quiroga, 2017 from Tanzania, mounted in Hoyer's medium (N–number of specimens/structures measured, RANGE refers to the smallest and the largest structure among all measured specimens; SD–standard deviation).

CHARACTER	N	RANGE		MEAN		SD	
		μm	*pt*	μm	*pt*	μm	*pt*
Body length	30	198–279	*803–1037*	244	*928*	20	*60*
Buccopharyngeal tube							
Buccal tube length	30	24.3–27.8	–	26.3	–	1.1	–
Stylet support insertion point	30	14.6–16.9	*58.7–60.9*	15.9	*60.3*	0.7	*0.6*
Buccal tube external width	30	1.7–2.2	*6.3–9.0*	2.0	*7.7*	0.1	*0.6*
Buccal tube internal width	30	0.8–1.2	*2.9–4.5*	1.0	*3.9*	0.1	*0.4*
Ventral lamina length	29	11.5–14.1	*45.1–51.8*	12.6	*48.0*	0.7	*1.7*
Placoid lengths							
Macroplacoid 1	30	1.6–2.6	*5.8–9.8*	2.1	*8.0*	0.2	*0.9*
Macroplacoid 2	30	1.3–2.0	*4.7–7.4*	1.7	*6.3*	0.2	*0.7*
Macroplacoid 3	30	1.3–2.1	*4.7–7.9*	1.7	*6.4*	0.2	*0.8*
Microplacoid	30	0.5–1.1	*1.9–4.2*	0.8	*2.9*	0.2	*0.6*
Macroplacoid row	30	6.1–8.1	*23.9–30.5*	7.1	*27.1*	0.5	*1.6*
Placoid row	30	7.4–10.1	*28.8–37.1*	8.4	*32.1*	0.6	*1.9*
Claw 1 lengths							
External primary branch	24	4.8–6.3	*19.1–23.7*	5.5	*21.1*	0.4	*1.2*
External secondary branch	14	3.4–5.0	*14.0–18.5*	4.3	*16.3*	0.4	*1.4*
Internal primary branch	23	4.7–5.7	*18.1–21.2*	5.2	*19.9*	0.3	*0.8*
Internal secondary branch	13	3.4–4.3	*12.8–16.2*	4.0	*15.0*	0.2	*0.9*
Claw 2 lengths							
External primary branch	24	5.1–6.2	*19.8–24.3*	5.7	*21.6*	0.3	*1.1*
External secondary branch	19	4.1–4.9	*15.0–18.1*	4.5	*16.9*	0.3	*0.8*
Internal primary branch	23	4.6–6.0	*18.7–22.6*	5.4	*20.6*	0.4	*1.1*
Internal secondary branch	17	3.5–4.7	*14.0–17.4*	4.1	*15.7*	0.3	*0.9*
Claw 3 lengths							
External primary branch	24	5.4–6.3	*20.4–24.5*	5.9	*22.4*	0.3	*0.9*
External secondary branch	17	4.1–4.9	*15.9–18.5*	4.5	*17.2*	0.2	*0.9*
Internal primary branch	24	5.1–6.2	*19.5–22.4*	5.6	*21.2*	0.3	*0.7*
Internal secondary branch	15	3.8–4.5	*14.3–17.1*	4.2	*16.1*	0.2	*0.8*
Claw 4 lengths							
Anterior primary branch	26	5.8–7.4	*20.9–27.6*	6.6	*24.9*	0.4	*1.5*
Anterior secondary branch	15	4.6–6.0	*16.5–22.1*	5.2	*19.5*	0.4	*1.6*
Posterior primary branch	26	6.1–7.7	*22.7–29.2*	7.0	*26.4*	0.4	*1.4*
Posterior secondary branch	17	4.6–6.1	*18.1–22.1*	5.4	*20.4*	0.4	*1.1*

20–30 min in thermomixer with constant 500 rpm. Then, tubes were incubated at 70 °C for 10 min and after cooling to room temperature, the supernatant was transferred to new 1.5 ml tubes and stored in −20 °C. Before the extraction, specimens were mounted in water slides and check under microscope to confirm their identification. We sequenced four DNA fragments: the small ribosome subunit (18S rRNA, nDNA), the large ribosome subunit (28S rRNA, nDNA), the internal transcribed spacer (ITS-2, nDNA), and the cytochrome oxidase subunit I (COI, mtDNA). All fragments were amplified using the primers listed in Table 1. For every PCR reaction, the solution contained 12.25 μl ddH2O, 2 μl 10X DreamTaq Green Buffer (Thermo Scientific™), 0.8 μl 10 mM dNTPs, 0.8 μl 10 μM forward primer, 0.8 μl 10 μM reverse primer, 0.15 μl DreamTaq DNA Polymerase (5U/μl; Thermo Scientific™) and 3.2 μl of genomic DNA extract. The PCR profile for amplification of 28S rRNA, ITS-2 and COI was as follow: 5 min initial denaturation at 95 °C, followed by 30 s denaturation at 95 °C, 90 s annealing at 51 °C, 60 s elongation at 72 °C for 35 cycles and 10 min of final elongation at 72 °C. For amplification of 18S rRNA the same profile was used with the exception of annealing temperature which was increased to 60 °C. The PCR products were controlled by 1.5% agarose gel electrophoresis stained with Midori Green (Nippon Genetics) and purified with the Enzymatic Post-PCR immediate Clean-up (EPPiC Fast; A&A Biotechnology). Sequencing reactions were carried out in a total volume of 10.0 μl containing: 1.0 μl 5 × buffer, 0.5 μl BrilliantDye® Terminator v3.1 (Life Technologies), 0.15 μl of a primer (10 pmol/μl), 2.0 μl of the purified PCR product, and 6.35 μl of ddH2O. Sequencing settings were: an initial denaturation at 96 °C for 1 min, followed by 25 cycles of denaturation at 96 °C for 10 s, annealing at 55 °C for 5 s, and elongation at 60 °C for 4 min. Sequencing products were then purified with the ExTerminator kit (A&A Biotechnology) and suspended in 25 μl of formamide. Sequencing products were read with the ABI 3130xl sequencer at the Molecular Ecology Lab, Institute of Environmental Sciences of the Jagiellonian University, Kraków, Poland. Sequences were processed in BioEdit ver. 7.2.5 (Hall 1999) and submitted to GenBank (for the accession numbers please see Table 2).

2.6. Comparative genetic analysis

For molecular comparisons, all published sequences of the four abovementioned markers for species of the genus *Minibiotus* were downloaded from GenBank (Table 2) except single 18S rRNA and

Table 6
Measurements [in μm] of selected morphological structures of the eggs of *Minibiotus pentannulatus* Londoño, Daza, Lisi & Quiroga, 2017 from Tanzania, mounted in Hoyer's medium (N–number of eggs/structures measured, RANGE refers to the smallest and the largest structure among all measured specimens; SD–standard deviation).

CHARACTER	N	RANGE	MEAN	SD
Diameter of egg without processes	30	50.2–65.4	58.6	3.6
Diameter of egg with processes	30	60.8–77.0	69.1	4.3
Process height	90	2.2–6.8	4.6	0.9
Process base width	90	2.6–5.4	3.8	0.5
Process base/height ratio	90	49%–214%	87%	26%
Distance between processes	90	0.9–2.4	1.7	0.3
Number of processes on the egg circumference	30	30–36	32.3	1.9

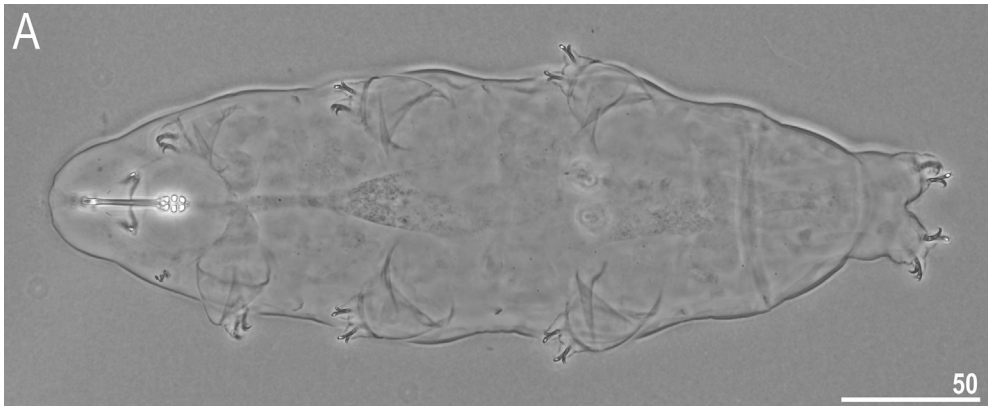

Fig. 1. ***Minibiotus ioculator*** **sp. nov.** – **habitus. (A)** Dorso-ventral projection (holotype, Hoyer's medium, PCM). Scale bars in μm.

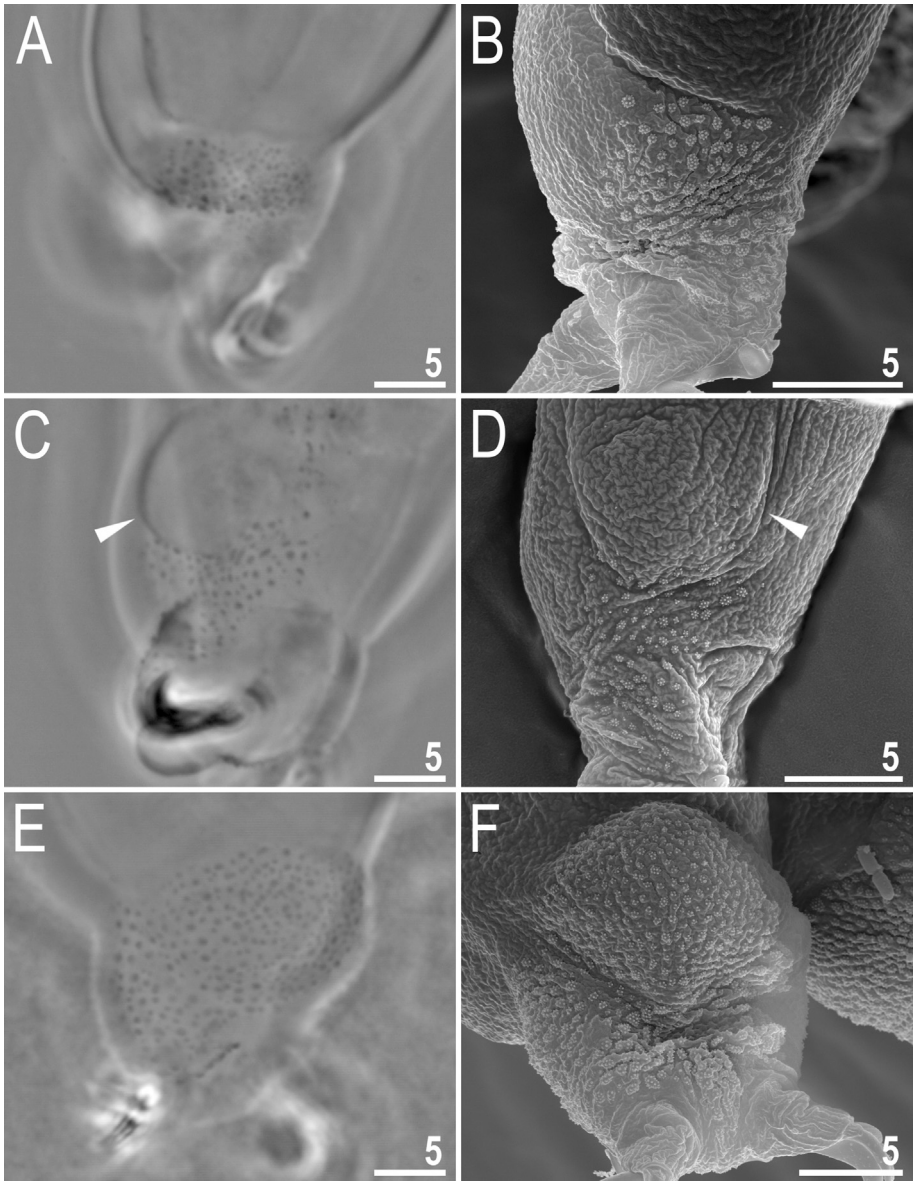

Fig. 2. ***Minibiotus ioculator*** **sp. nov.** – **cuticular structures on legs. (A–B)** External granulation on leg III seen in PCM (A) and SEM (B) (paratypes). **(C–D)** Internal granulation on leg III and a cuticular bulge resembling a pulvinus seen in PCM (C) and SEM (D) (paratypes). **(E–F)** Granulation on leg IV seen in PCM (E) and SEM (F) (paratypes). Filled, flat arrowheads indicate the cuticular bulge. Scale bars in μm.

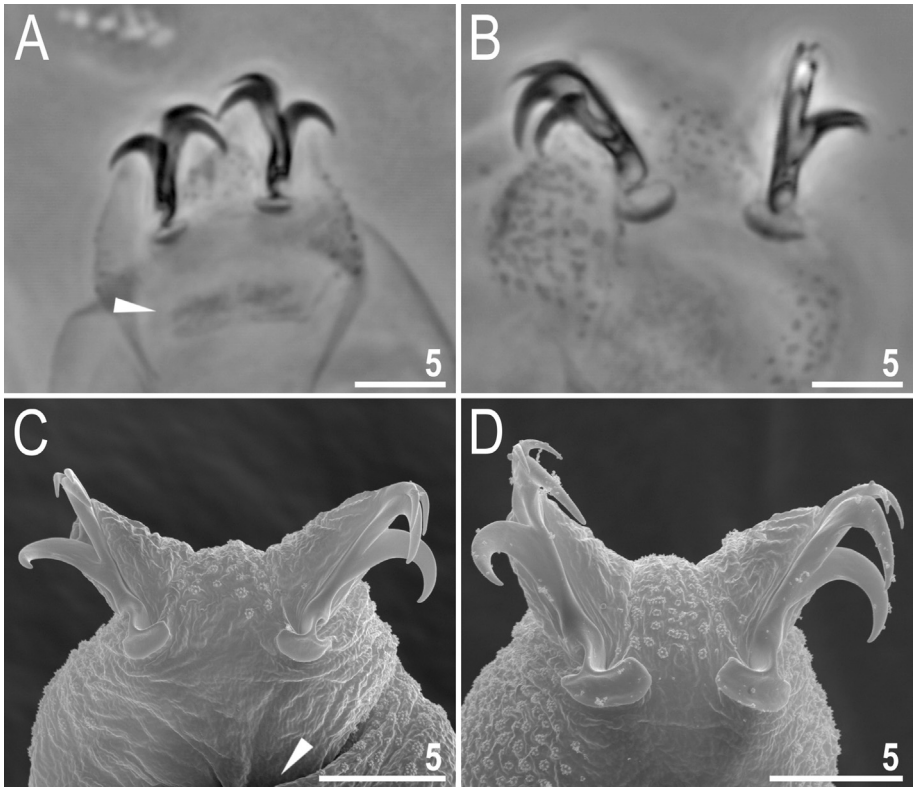

Fig. 3. ***Minibiotus ioculator*** **sp. nov. – claws (paratypes). (A–B)** Claws I (A) and IV (B) seen in PCM. **(C–D)** Claws I (C) and IV (D) seen in SEM. Filled flat arrowheads indicate double muscle attachments under the claws. Scale bars in μm.

28S rRNA sequences (MH079468 and MH079492) published by Guil et al. (2019) as they represent a non-homologous fragment. The sequences were aligned using the default settings (in the case of ITS-2 and COI) and the Q–INS–I method (in the case of ribosomal markers: 18S rRNA, 28S rRNA) of MAFFT version 7 (Katoh et al. 2002; Katoh & Toh 2008) and manually checked against non-conservative alignments in BioEdit. Then, the aligned sequences were trimmed to: 760 (18S rRNA), 687 (28S rRNA), 437 (ITS-2), 620 (COI) bp. All COI sequences were translated into protein sequences in MEGA7 version 7.0 (Kumar et al. 2016) to check against pseudogenes. Uncorrected pairwise distances were calculated using MEGA7 and are provided as supplementary materials (SM.03).

3. Results

3.1. Taxonomic account of the new species

Phylum: Tardigrada Doyère 1840.
Class: Eutardigrada Richters 1926.
Order: Macrobiotoidea Guil et al. 2019.
Family: Macrobiotidae Thulin 1928.
Genus: *Minibiotus* R.O. Schuster, 1980 (in Schuster et al. 1980).

3.2. Minibiotus ioculator sp. nov.

(Tables 3 and 4, Figs. 1–8).

3.2.1. Material examined

99 animals (including 4 simplex), and 31 eggs. Specimens mounted on microscope slides in Hoyer's medium (84 animals + 21 eggs), fixed on SEM stubs (10 + 10 + 2 buccal apparatuses), and processed for DNA sequencing (3 + 0).

3.2.2. Type locality

33°58′58.44″S, 20°42′17.88″E; 295 m asl: Republic of South Africa: Tradouw Pass located in Western Cape; lichen on rock in the forest; coll. 7 September 2018 by Witold Morek and Bartłomiej Surmacz.

3.2.3. Type depositories

Holotype (slide ZA.274.23 with 10 paratypes) and 68 paratypes (slides: ZA.274.*, where the asterisk can be substituted by any of the following numbers 19, 22, 25–26; SEM stub: 18.14) and 23 eggs (slides: ZA.274.*: 20–21; SEM stub: 18.14) are deposited at the Institute of Zoology and Biomedical Research, Jagiellonian University, Gronostajowa 9, 30-387, Kraków, Poland and 14 paratypes (slide: ZA.274.*: 24) and 8 eggs (slides: ZA.274.*: 18) are deposited in the Natural History Museum of Denmark, University of Copenhagen, Universitetsparken 15, DK-2100 Copenhagen Ø, Denmark.

3.2.4. Etymology

The name refers to morphology of processes on the egg shell which resembles a hat of a royal jester. From Latin "jester" = "*ioculator*".

3.2.5. Description of the new species

3.2.5.1. Animals (measurements and statistics in Table 3). Body whitish but transparent after fixation in Hoyer's medium (Fig. 1A). Eyes present in live animals as well as in specimens mounted in Hoyer's medium. Body cuticle smooth without pores and granulation, however clearly visible patches of big and dense granulation on all legs present (Fig. 2A–F). The granulation on legs I–III consists of two wide patches on the external and internal leg surface which are joined by narrow band of granulation situated on the anterior leg surface (Fig. 2A–D and 3A, C). The granulation on legs IV consists of a

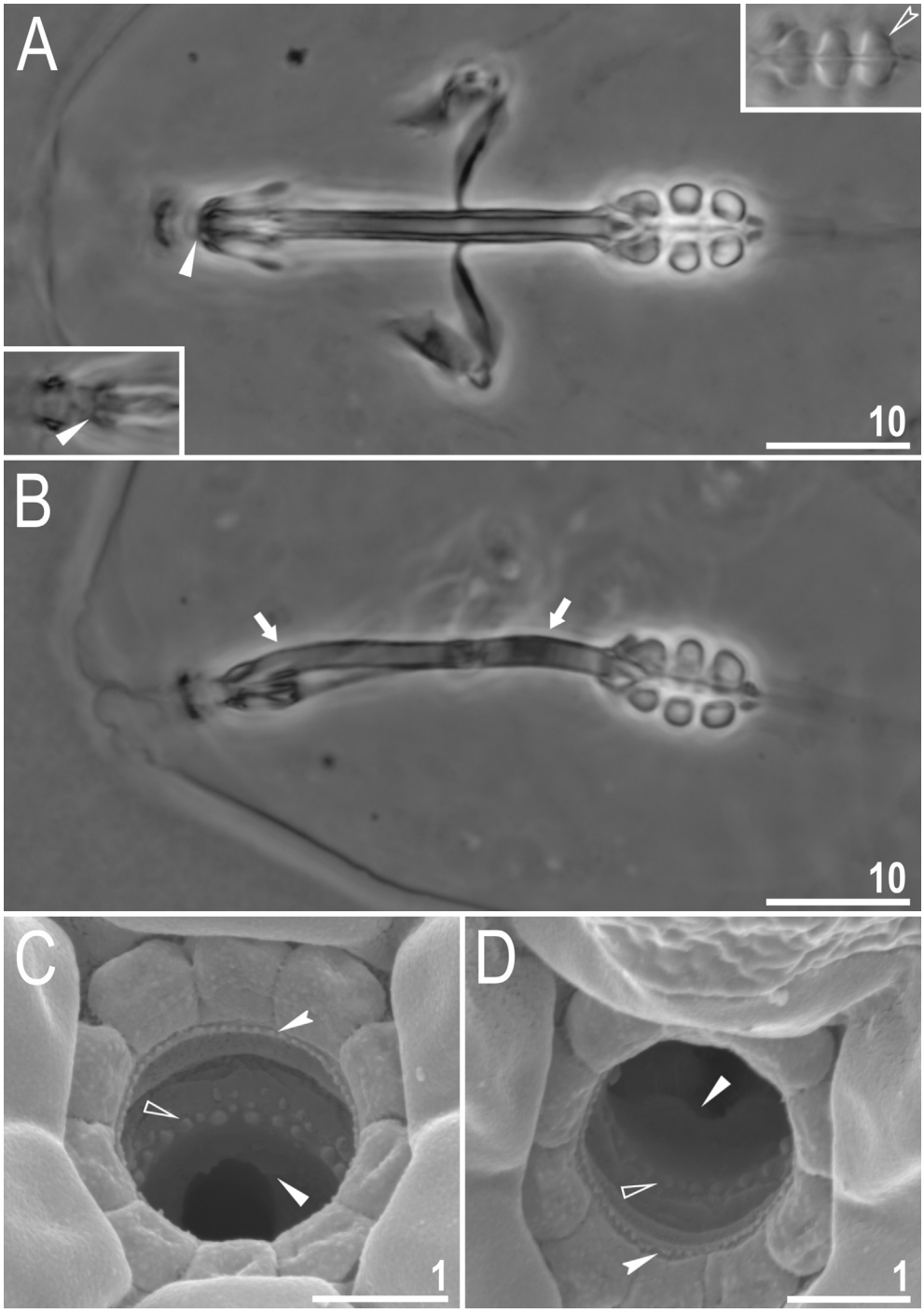

Fig. 4. ***Minibiotus ioculator*** **sp. nov.** – **buccal apparatus and the oral cavity armature. (A)** Dorsal view of the entire buccal apparatus (PCM), lower and upper inserts show ventral views of the oral cavity armature (PCM) and macroplacoids (NCM), respectively (all holotype). **(B)** Lateral view of the entire buccal apparatus (PCM) with the anterior and the posterior bend of the buccal tube. **(C–D)** The oral cavity armature of a single paratype seen in SEM from different angles showing dorsal (B) and ventral (C) views. Filled indented arrowheads indicate teeth of the first band, empty flat arrowheads indicate teeth of the second band whereas filled flat arrowheads indicate the third band of teeth, arrows indicate the anterior and the posterior bend of the buccal tube. Scale bars in μm.

continuous and uniform patch which covers lateral and dorsal leg surfaces (Fig. 2E and F and 3B, D). A cuticular bulge/fold (pulvinus) is present on the internal surface of legs I–III (Fig. 2C and D).

Claws slender, of the *hufelandi* type (Fig. 3A–D). Primary branches with distinct accessory points, a common tract, and with an evident stalk connecting the claw to the lunula (Fig. 3A–D). Lunulae smooth on all legs (Fig. 3A–D). Cuticular bars under claws absent. Double muscle attachments faintly marked under LCM but clearly visible under SEM (Fig. 3A, C).

Mouth antero-ventral followed by ten peribuccal papulae (Fig. 4A–C; but see also Discussion). Bucco-pharyngeal apparatus of the *Minibiotus* type (Figs. 4A and 5A–C) with an anterior and a

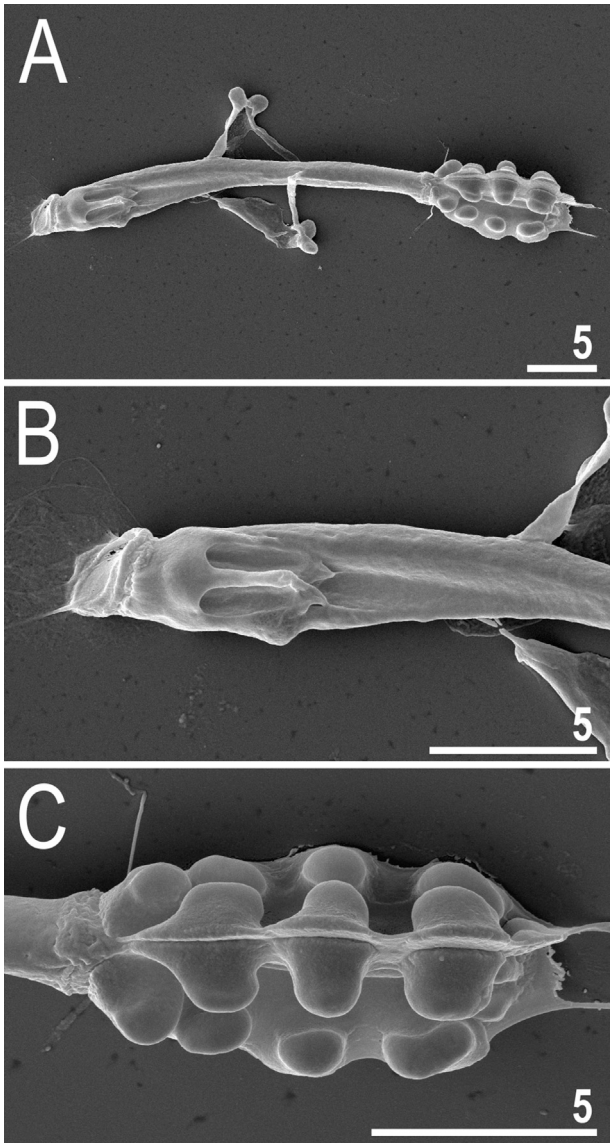

Fig. 5. ***Minibiotus ioculator*** **sp. nov. – buccal apparatus seen in SEM. (A)** Entire buccal apparatus. **(B)** Magnification of the anterior portion of the buccal apparatus. **(C)** Magnification of the placoids. Scale bars in μm.

posterior bend clearly visible in laterally positioned specimens under LCM (Fig. 4B). Under LCM, only the third band of teeth is faintly visible (Fig. 4A). However, in SEM all three bands of teeth are visible, with the first band being situated at the base of peribuccal papulae and composed of a single row of small cone-shaped teeth fused to form a continuous, slightly serrated ring ridge around the oral cavity (Fig. 4C and D). The second band of teeth is situated between the ring fold and the third band of teeth and comprises one row of globular-shaped teeth, with occasional additional smaller teeth placed closer to the ring fold (Fig. 4C and D). The teeth of the third band are located in the posterior portion of the oral cavity, between the second band of teeth and the buccal tube opening (Fig. 4A, C–D). The third band of teeth is discontinuous and divided into the dorsal and the ventral portions. Under LCM, the teeth of both portions form a single, faintly visible transverse ridge, with dorsal ridge being continuous and ventral slightly indented (Fig. 4A). In SEM, both dorsal and ventral teeth are also clearly distinct and each is fused into a single ridge (Fig. 4C and D). Under SEM, both dorsal and ventral ridges have two clearly visible peaks with sharpened and flattened ends, respectively (Fig. 4C and D). Pharyngeal bulb spherical, with large triangular apophyses, three granular macroplacoids and a triangular small microplacoid placed very close to the third macroplacoid (Figs. 4A and 5C). The macroplacoid length sequence $2 < 3 < 1$. The first macroplacoid narrowed anteriorly (Figs. 4A and 5C). All macroplacoids without constrictions (Figs. 4A and 5C).

3.2.5.2. Eggs (measurements and statistics in Table 4). Laid freely, white, spherical or slightly ovoid (Fig. 6A and B and 7A). The surface between processes smooth with depressions between processes faintly visible in LCM and clearly visible in SEM (Fig. 6B–F and 7A–F). In SEM, these depressions are perforated by micropores (Fig. 7B and C). However, depressions with micropores can sometimes be not visible due to particles of dirt/mucus which sometimes accumulate within the depressions (Fig. 7D–F). Processes are conical with a slender trunk and with apex often split into a few apices (Fig. 6C–F and 7D–F). The most common and characteristic appearance is a bifurcated process which resembles a hat of a medieval European royal jester (Fig. 6C–F and 7D). Process apices are covered by granules which are faintly visible in LCM but are clearly identifiable in SEM (Fig. 6C–F and 7D–F). Only occasionally, singular bubble-like structures can be seen inside the terminal portion of the processes (Fig. 6C–F). Sometimes, under LCM, the margins of processes bases seem to be serrated and surrounded by a crown of small thickenings (Fig. 6C–F) which are most probably internal strengthening structures stabilising the processes within the chorion as in other Macrobiotidae species (e.g. see Michalczyk & Kaczmarek 2003). In SEM, these structures are not visible in intact eggs (Fig. 7D–F).

3.2.5.3. Reproduction. The new species is dioecious. Although no spermathecae filled with sperm have been found in gravid females on the freshly prepared slides, the testis in males, filled with spermatozoa, was clearly visible under LCM up to 24 h after mounting in Hoyer's medium (Fig. 8A). The new species does not exhibit sexual dimorphism such as lateral gibbosities on legs IV in males.

3.2.5.4. Phenotypic differential diagnosis. By smooth body cuticle without granulation and pores as well as by eggs with conical processes, the new species is similar to the following six *Minibiotus* species: *M. allani* (Murray, 1913), *M. crassidens* (Murray, 1907), *Minibiotus aquatilis* Claxton, 1998, *Minibiotus hispidus* Claxton, 1998, *Minibiotus macularus* Pilato & Claxton, 1988, *Minibiotus milleri* Claxton, 1998. However, it differs specifically from:

- *M. allani*, reported only from the type locality in Kenya (Murray 1913), by: the presence of eyes (eyes absent in *M. allani*), the presence of granulation on all legs (granulation absent or not visible under light microscope in *M. allani*) and a different egg processes morphology (egg processes with slender trunks and endings split into stout arms with the most common and characteristic being division into two often curved arms which resemble a hat of a royal jester in the new species vs. egg processes with stouter trunks and endings split into several thin, flexible filaments in *M. allani*).
- *M. crassidens*, reported from five African countries: Angola (da Cunha & do Nascimento 1964), Democratic Republic of Congo (Teunissen 1938), Kenya (Murray 1913), Republic of South Africa (Murray 1907, 1913), and Uganda (Murray 1913), by: the presence of eyes (eyes absent in *M. crassidens*) and a different egg processes morphology (egg processes with slender trunks and endings split into stout arms with the most common and

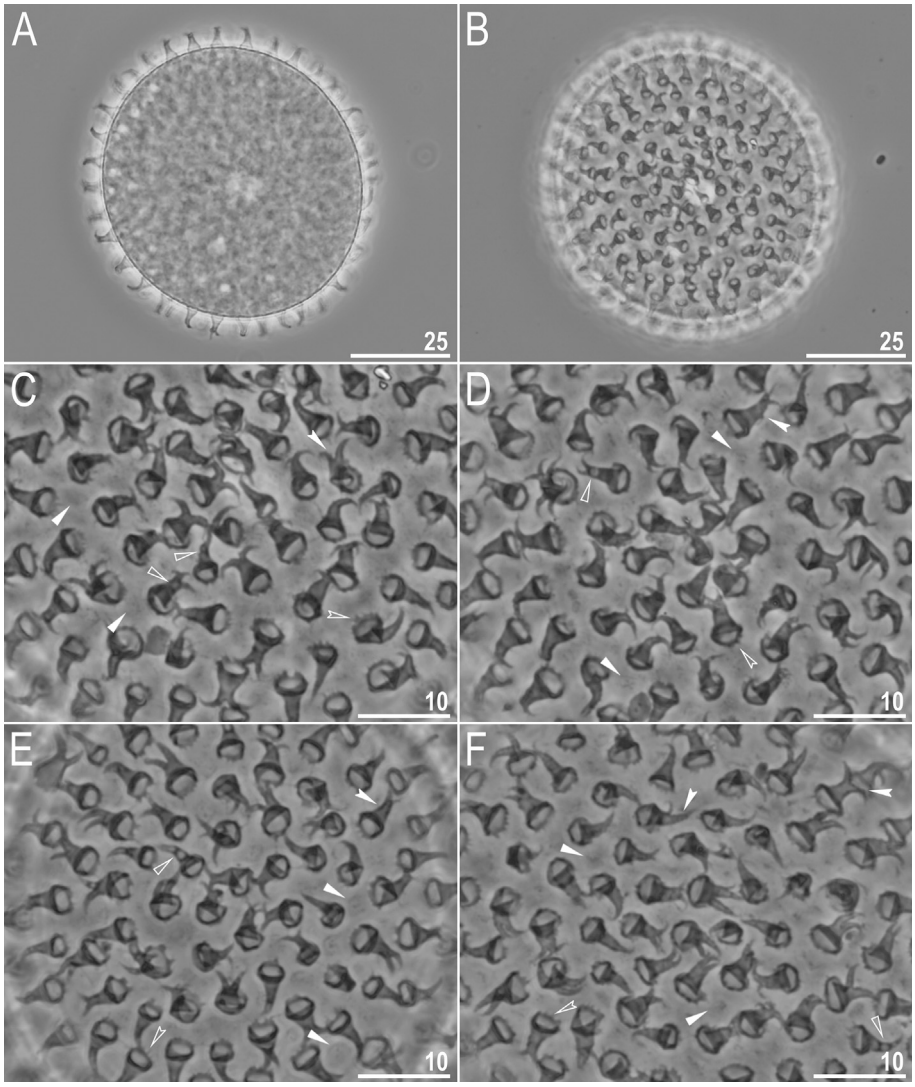

Fig. 6. *Minibiotus ioculator* sp. nov. – eggs seen in PCM. (A) Midsection under a 400 × magnification. **(B)** Surface under a 400 × magnification. **(C–E)** Details of egg under a 1000 × magnification. Filled flat arrowheads indicate faintly visible depressions on the egg surface between the processes, empty flat arrowheads indicate singular bubble-like structures, filled indented arrowheads indicate faintly visible granules on the processes whereas empty indented arrowheads indicate internal thickenings (attachments/sutures) at the process bases. Scale bars in μm.

characteristic being division into two often curved arms which resemble a hat of a royal jester in the new species vs. egg processes with undivided ending which is elongated into flexible one long flexible filament in *M. crassidens*) and a less denser distribution of process on the egg surface (the processes densely distributed, almost in contact with each other so that the egg surface between processes is hardly visible in *M. crassidens*);

- *M. aquatilis*, reported from several localities in Australia and Tasmania (Claxton 1998), by: the presence of smooth lunules IV (lunules IV dentate in *M. aquatilis*), a different morphology of egg processes (egg processes with slender trunks and endings split into stout arms with the most common and characteristic being division into two often curved arms which resemble a hat of a royal jester in the new species vs. egg processes long with slender trunks elongated usually into one and only sometimes several flexible, hair-like filaments often with one line of small bauble-like structures visible inside in *M. aquatilis*), a different morphology of egg surface between processes (smooth surface with depressions faintly visible under LCM vs. the surface between processes covered by large dark dots arrange with single line around processes in *M. aquatilis*), and by shorter egg processes (4.5–7.9 μm in the new species vs. 11.0–12.5 μm in *M. aquatilis*).
- *M. hispidus*, reported only from Australia and New Zealand (Claxton 1998), by: a different morphology of egg processes (egg processes with slender trunks and endings split into stout arms with the most common and characteristic being division into two often curved arms which resemble a hat of a royal jester in the new species vs. egg processes in shape of small cones with greatly elongated, undivided endings in *M. hispidus*), a different morphology of egg surface between processes (smooth surface with depressions faintly visible under LCM vs. the surface between processes covered by small pores uniform in size with a distinct ring of pores surrounding each process in *M. hispidus*), and by a smaller number of process on the egg circumference (30–32 in the new species vs. 48 in *M. hispidus*).
- *M. macularus*, reported from several localities in Australia and one in New Zealand (Pilato & Claxton 1988; Claxton 1998), by: the presence of smooth lunules IV (lunules IV dentate in

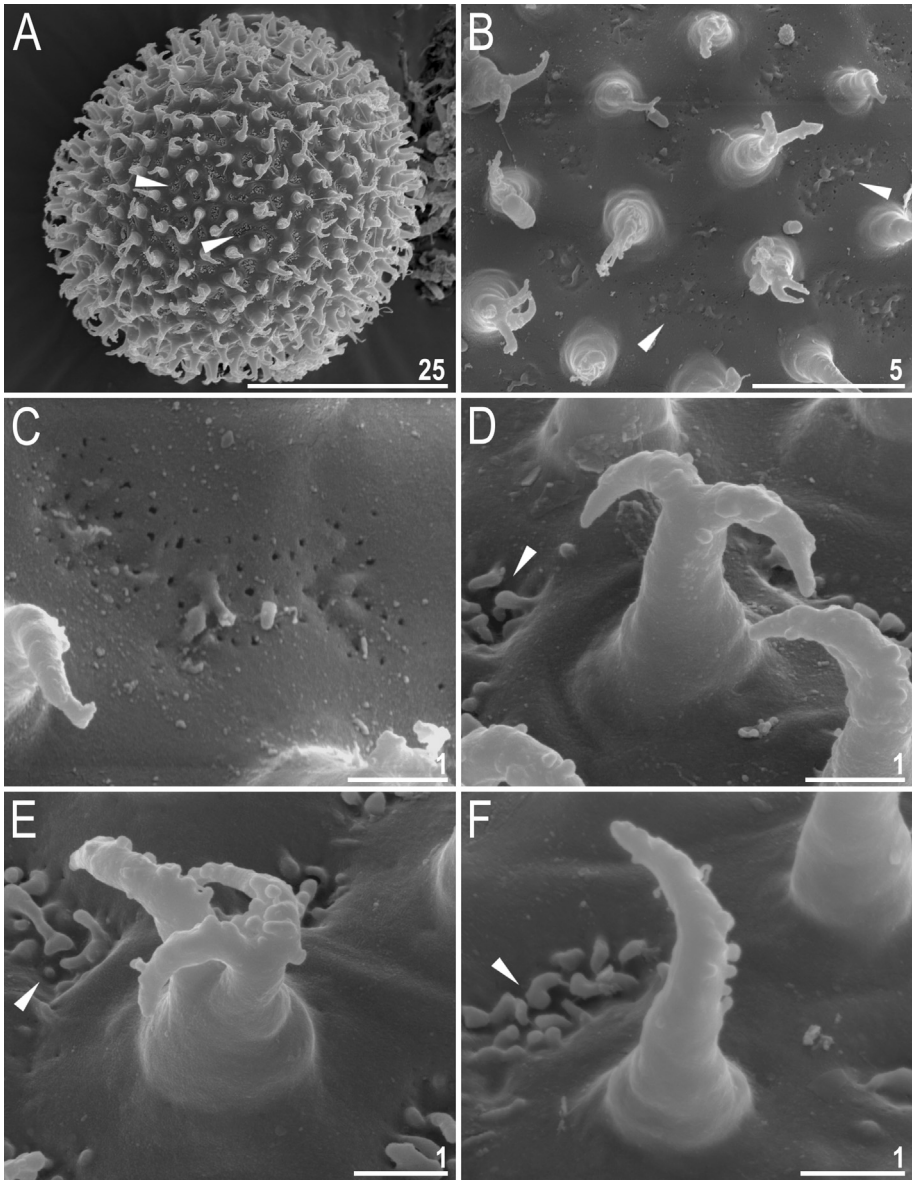

Fig. 7. ***Minibiotus ioculator*** **sp. nov.** – **egg chorion seen in SEM. (A)** Entire egg. **(B)** Details of the egg surface. **(C)** Magnification of a depression on the egg surface between the processes. **(D–F)** details of the processes. Filled flat arrowheads indicate depressions present on the egg surface between the processes. Please note that on A and D–F the depressions are covered by dirt. Scale bars in μm.

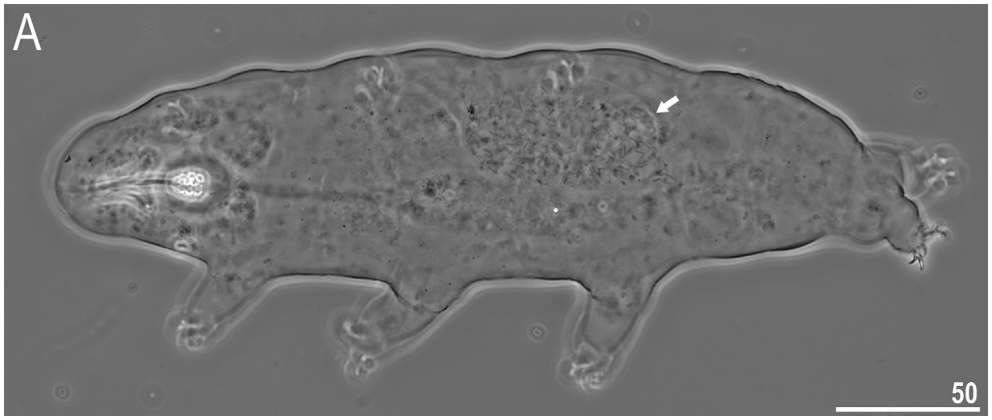

Fig. 8. ***Minibiotus ioculator*** **sp. nov.** – **reproduction. (A)** Male testis (indicated by the arrow) seen in PCM, with visible spermatozoa in a male freshly mounted in Hoyer's medium. Scale bars in μm.

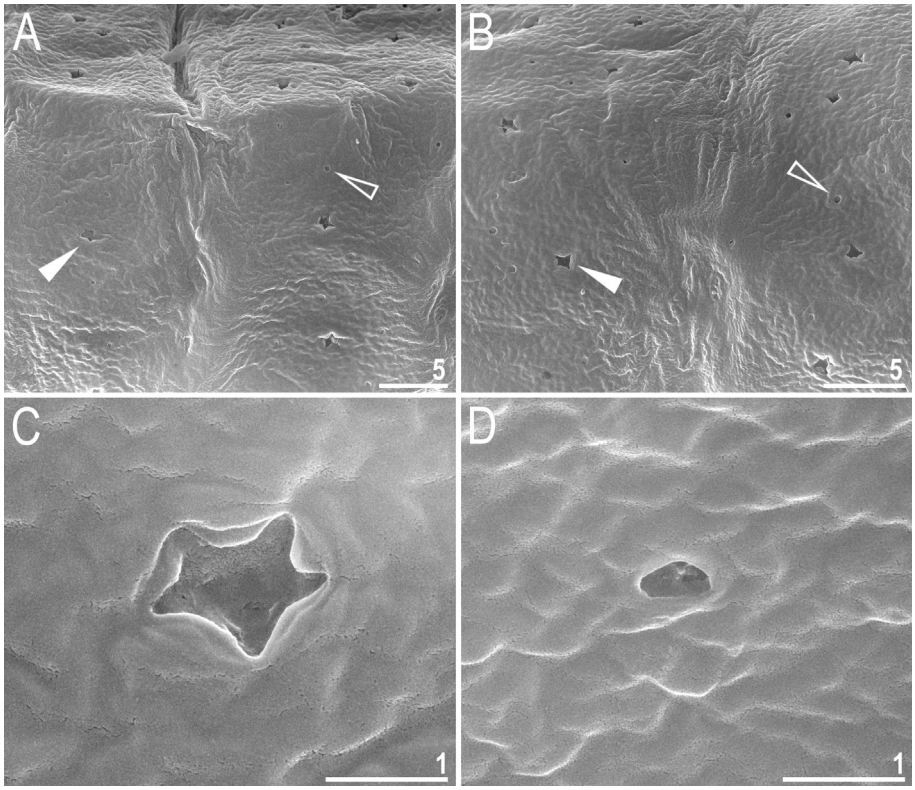

Fig. 9. ***M. pentannulatus*** **Londoño et al., 2017 from Tanzania – cuticular pores seen in SEM. (A–B)** Cuticular pores on the dorsal cuticle at the level of leg I (A) and leg III (B). **(C–D)** Magnification of star-shaped (C) and circular (D) pores. Scale bars in μm.

M. maculartus), a different morphology of egg processes (egg processes with slender trunks and endings split into stout arms with the most common and characteristic being division into two often curved arms which resemble a hat of a royal jester in the new species vs. wide conical processes with pointed apices with 8–9 longitudinal ridges extending from the processes base and joying the processes to the egg surface in *M. maculartus*), a different morphology of egg surface between processes (smooth surface with depressions faintly visible under LCM vs. the surface covered by irregularly distributed dark dots irregular in size and shape in *M. maculartus*), a shorter egg processes (4.5–7.9 μm in the new species vs. all processes about 11 μm in *M. maculartus*), a narrower processes bases (2.1–4.2 μm in the new species vs. all processes bases about 11 μm in *M. maculartus*), and by a higher number of process on the egg circumference (30–32 in the new species vs. 16 in *M. maculartus*).

- *M. milleri*, reported only from two localities in Australia (Claxton 1998), by: a different macroplacoid length sequence (2 < 3<1 in the new species vs. 1< 2<3 in *M. milleri*), a different morphology of egg processes (egg processes with slender trunks and endings split into stout arms with the most common and characteristic being division into two often curved arms which resemble a hat of a royal jester in the new species vs. processes in shape of long cones, tapering to blunt tip, rarely bifurcated with rough surface of tapering portion appearing as transverse lines and with indented bases enclosed within in membrane in *M. milleri*), a different morphology of egg surface between processes (smooth surface with depressions faintly visible under LCM vs. the surface slightly striated in *M. milleri*), a shorter egg full diameter (66.2–81.1 μm in the new species vs. 90.0–98.0 μm in *M. milleri*), a shorter egg processes (4.5–7.9 μm in the new species vs. 10.0–14.0 μm in *M. aquatilis*), and by a slightly smaller number of process on the egg circumference (30–32 in the new species vs. 20–30 in *M. milleri*).

3.2.5.5. Genetic differential diagnosis. The ranges of uncorrected genetic p-distances between the new species and the few *Minibiotus* species, for which sequences are available from GenBank, are as follows:

18S rRNA: 2.0–4.5% (3.7% on average), with the most similar being *M. pentannulatus* from Tanzania (MT023999) and the least similar being unidentified *Minibiotus* species from England (EU266934);

28 rRNA: comparison with only two species: 7.2 and 7.3% difference with *M. pentannulatus* from Tanzania (MT024042 and MT024043, respectively) and 10.1% difference with *M. gumersindoi* from Spain (FJ435761);

ITS-2: comparison with only one species: 19.2% difference with *M. pentannulatus* from Tanzania (MT024001);

COI: comparison with only two species: 21.1% difference with *M. pentannulatus* from Tanzania (MT023413 and MT023414) and 23.9% difference with *M. gumersindoi* from Spain (FJ435803);

3.3. *Minibiotus pentannulatus* Londoño, Daza, Lisi & Quiroga, 2017

The population of *Minibiotus* species found in Tanzania and examined in this study was identified as *M. pentannulatus* based on the original description and new LCM microphotographs of type material. Data collected for this population allowed to amend the species description by providing more accurate morphological details from LCM and SEM as well as DNA barcodes for molecular species identification.

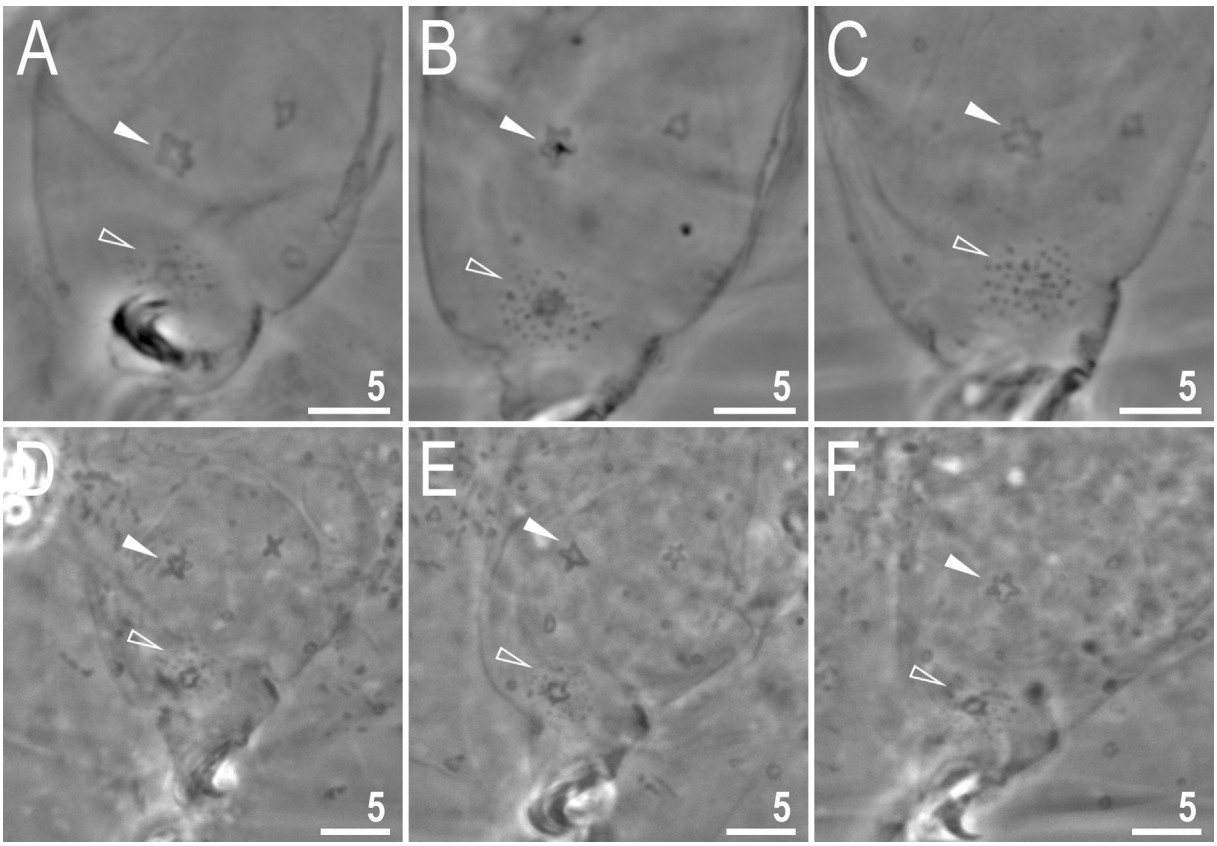

Fig. 10. ***M. pentannulatus*** **Londoño et al., 2017 from Tanzania and Colombia – cuticular structures on the external leg surface. (A–C)** External surface of leg I (A), II (B) and III (C) of the same animal from the Tanzanian population. **(D–F)** External surface of leg I (A), II (B) and III (C) of the same animal from the Colombian population (a paratype). Empty arrowheads indicate the patch of leg granulation with a cuticular pore in the centre whereas filled arrowheads indicate the big star-shaped cuticular pore always present above the granulation. Scale bars in μm.

3.3.1. Material examined

83 animals (including 6 simplex), and 46 eggs. Specimens mounted on microscope slides in Hoyer's medium (60 animals + 34 eggs), fixed on SEM stubs (20 + 9), and processed for DNA sequencing (3 + 3).

3.3.2. Locality

7°49′25″S, 36°49′32″E, 2050 m asl: Tanzania: Udzungwa Mts. National Park near the Mwanihana Peak; lichen from branches of a bush; coll. on 16 August 2016 by Thomas Pape.

3.3.3. Material depositories

69 animals (slides: TZ.027.*, where the asterisk can be substituted by any of the following numbers 23–25, 28–31; SEM stubs: 14.02, 19.20) and 36 eggs (slides: TZ.027.*: 32–35; SEM stub: 14.02) are deposited at the Institute of Zoology and Biomedical Research, Jagiellonian University, Gronostajowa 9, 30-387, Kraków, Poland and 11 animals (slides: TZ.027.*: 26–27) and 7 eggs (slide: TZ.027.*: 36) are deposited in the Natural History Museum of Denmark, University of Copenhagen, Universitetsparken 15, DK-2100 Copenhagen Ø, Denmark.

3.3.4. Amended description

3.3.4.1. Animals (measurements and statistics in Table 5). Both types of cuticular pores (star-shaped and circular) reported in the original description are also obvious in SEM (Fig. 9A–D). The granulation on legs I–III was overlooked in the original description. In both populations the granulation is present on the external surface of legs I–III as a single small patch well visible in LCM (Fig. 10A–F) and in SEM (Fig. 11A, C). Moreover, a clear pattern of pore arrangement on legs I–III is also always present with one smaller star-shaped pore present in the centre of granulation patch and bigger star-shaped pore present above (Fig. 10A–F). The SEM analysis additionally confirmed this pattern revealing at the same time also a pulvinus on the internal surface of legs I–III (Fig. 11A–D). Under SEM, the granulation on all legs consist of microgranule aggregations being the most obvious on legs IV (Fig. 11 A, C, E–F). The SEM analysis also confirmed that lunules on all legs are smooth (Fig. 11E and F). Bucco-pharyngeal apparatus of the *Minibiotus* type with the anterior and the posterior bend clearly visible in laterally positioned specimens under LCM (Fig. 12A). A cuticular fold with a pore in the centre is present just above the mouth opening and visible well under LCM (only in laterally positioned specimens) and under SEM (Fig. 12A and B). Mouth antero-ventral followed by ten short peribuccal papulae (Fig. 12B–D; but see also Discussion). As stated in the original description, the oral cavity armature is invisible under LCM. However, the SEM analysis confirmed the presence of teeth in the oral cavity. The oral cavity armature comprises three bands of teeth, with the first band being situated at the base of peribuccal lamellae and composed of a single row of small cone-shaped teeth fused to form a continuous, slightly serrated ring ridge around the oral cavity (Fig. 12C). The second band of teeth comprises one row of globular-shaped teeth with some smaller cone-shaped teeth distributed unevenly on the ring fold (Fig. 12C and D). The teeth of the third band are located within the posterior portion of the oral cavity, between the second band of teeth and the buccal tube

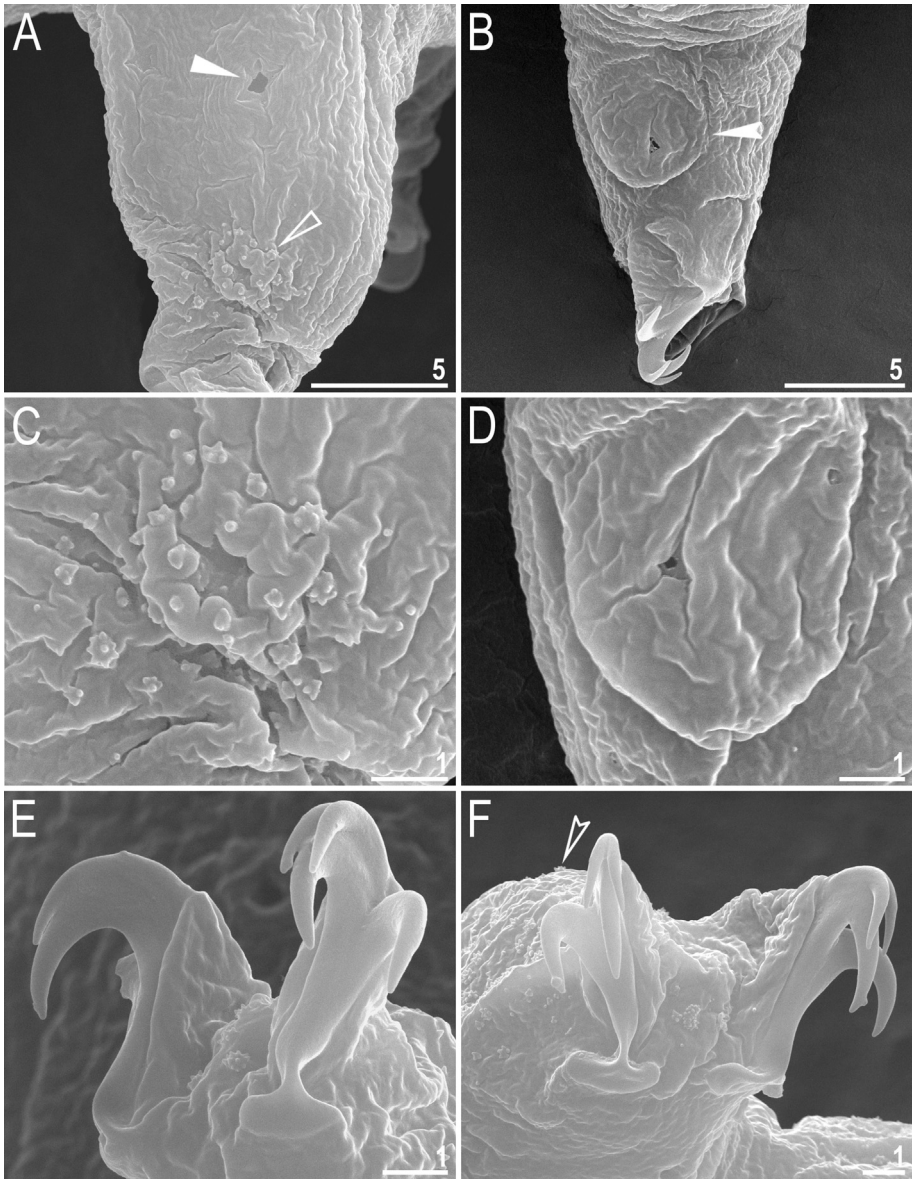

Fig. 11. ***M. pentannulatus*** **Londoño et al., 2017 from Tanzania – cuticular structures on legs and claws seen in SEM. (A–B)** External and internal surface of leg III (A) and II (B) respectively. **(C)** Magnification of granulation on leg III. **(D)** Magnification of the pulvinus on leg II. **(E–F)** Claws II (E) and IV (F). The empty flat arrowhead indicates the patch of leg granulation with a cuticular pore in the centre, the filled flat arrowhead indicates the big star-shaped cuticular pore always present above the granulation, the filled indented arrowhead indicates the pulvinus whereas the empty indented arrowhead indicates granulation on leg IV. Scale bars in μm.

opening (Fig. 12C), but only the dorsal portion of the third band of teeth is present (Fig. 12C and D). This portion is composed of three evidently separated, sharp cone-shaped teeth (Fig. 12C).

3.3.4.2. Eggs (measurements and statistics in Table 6). In the original description, the morphology of the egg ornamentation was reported based on a single egg. The egg shell ornamentation in the Tanzanian population conforms to that in the original description (Fig. 13A–F). The low sample size in the original description led Londoño et al. (2017) to assume that egg processes always exhibit 5 latitudinal annulations, but the analysis of a larger number of eggs showed that number of annulation on egg process varies from 4 to 6 (Fig. 13A–F and 14A–F). Under SEM, the annulations are seen as a laminal rings with serrated/granulated margins surrounding the processes (Fig. 14A–F). Both LCM and SEM analysis confirmed that the chorion surface between the process is smooth, however we noted also the presence of internal strengthening thickenings at the processes bases which stabilise them within the chorion layers as in other Macrobiotidae species (Fig. 13C–F and 14C–D). The microgranulation is present on the egg chorion surface under the processes, however it is visible only in SEM and only when processes are broken or detached from the chorion surface Fig. 14C and D).

3.3.4.3. Reproduction. Neither testis in males nor spermathecae filled with sperm in gravid females have been found on the freshly prepared slides. Also, specimens of the Tanzanian population did not exhibit sexual dimorphism such as lateral gibbosities on legs IV. Thus, most likely the species is parthenogenetic.

3.3.4.4. Genetic comparisons. The 18S rRNA and ITS-2 exhibited single haplotypes, but in 28S rRNA and COI, two haplotypes were found (Table 2), with p-distances of 0.1% and 2.1%, respectively. The ranges of uncorrected genetic p-distances between the Tanzanian

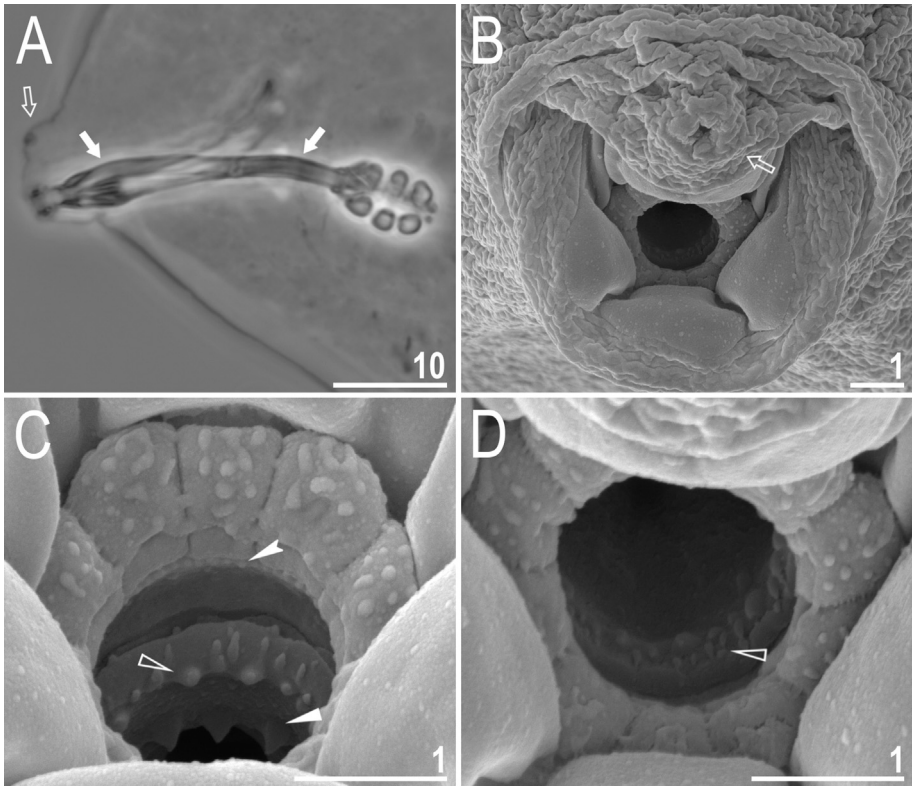

Fig. 12. ***M. pentannulatus*** **Londoño et al., 2017 from Tanzania – buccal apparatus and the oral cavity armature. (A)** Lateral view of the entire buccal apparatus (PCM) with the anterior and the posterior bend of the buccal tube. **(B)** Mouth opening visible in SEM. **(C–D)** The oral cavity armature of a single specimen seen in SEM from different angles showing dorsal (C) and ventral (D) views. Filled arrows indicate the anterior and the posterior bend of the buccal tube, empty arrows indicate the cuticular fold above the mouth opening with a central pore, filled indented arrowheads indicate teeth of the first band, empty flat arrowheads indicate teeth of the second band whereas filled flat arrowheads indicate the third band of teeth. Scale bars in μm.

M. pentannulatus and other *Minibiotus* species, for which sequences are available from GenBank, are as follow s:

18S rRNA: 2.0–4.0% (3.3% on average), with the most similar being *M. ioculator* **sp. nov.** from the Republic of South Africa (MT023998) and the least similar being unidentified species of the *M. intermedius* group from Italy (HQ604980);

28S rRNA: comparison with only two species: 7.2 and 7.3% difference with *M. ioculator* **sp. nov.** from the Republic of South Africa (MT024041) and 12.2 and 12.3% difference with *M. gumersindoi* from Spain (FJ435761);

ITS-2: comparison with only one species: 19.2% difference with *M. ioculator* **sp. nov.** from the Republic of South Africa (MT024000);

COI: comparison with only two species: 21.1% difference with *M. ioculator* **sp. nov.** from the Republic of South Africa (MT023412) and 23.9–24.4% difference with *M. gumersindoi* from Spain (FJ435803).

4. Discussion

Minibiotus was established 40 years ago by Schuster et al. (1980) who extracted several species from the genus *Macrobiotus* that were characterised by uniform morphology. Initially, however, the erection of *Minibiotus* was not commonly accepted and it was met with criticism by Pilato (1982) and Ramazzotti & Maucci (1983) who treated this genus invalid because they considered its diagnosis vague. Nevertheless, with time, the genus was eventually accepted and it currently comprises nearly fifty species. The first and so far the only revision of the genus by Claxton (1998) included descriptions of numerous new species, aiding species identification and further descriptions. Although the taxonomic status of *Minibiotus* is no longer challenged, the extreme morphological diversity within the genus presented by Claxton (1998) and later species descriptions clearly indicate that *Minibiotus* is likely to hold at least several distinct evolutionary lineages that could potentially be described as separate genera (Stec et al. 2015). Specifically, *Minibiotus* comprises species with two and three macroplacoids in the pharynx or species without and with pores and the latter can be further divided into species with solely circular pores and species with a mixture of circular and star-shaped pores. Recent phylogenetic works show that morphological traits such as the number of macroplacoids and even their shape and spatial arrangement or the presence of cuticular pores are stable at the genus level (e.g. see the following genera that were established with integrative data in which the macroplacoid number and morphology were used as major diagnostic characters: *Paramacrobiotus*, *Mesobiotus* or *Pilatobius*). Apart from *Minibiotus*, there are also other tardigrade genera that were erected before the molecular phylogenetics era, solely with morphological data and that comprise species with varying numbers of macroplacoids (e.g. *Doryphoribius* and *Adropion*). Importantly, however, their phylogenies have not been thoroughly studied, thus it is likely that these genera are not monophyletic either (see Gąsiorek et al. 2019). Moreover, some of the *Minibiotus* species originally described with two macroplacoids have recently been transferred to the *Macrobiotus hufelandi* group after a careful PCM analysis (i.e. *M. acadianus* and *M. julianae* in Stec et al., 2015). Similarly, in all tardigrade genera that were verified by methods of molecular phylogenetics, cuticle is either porous or poreless, suggesting that this trait is typically conserved at a genus

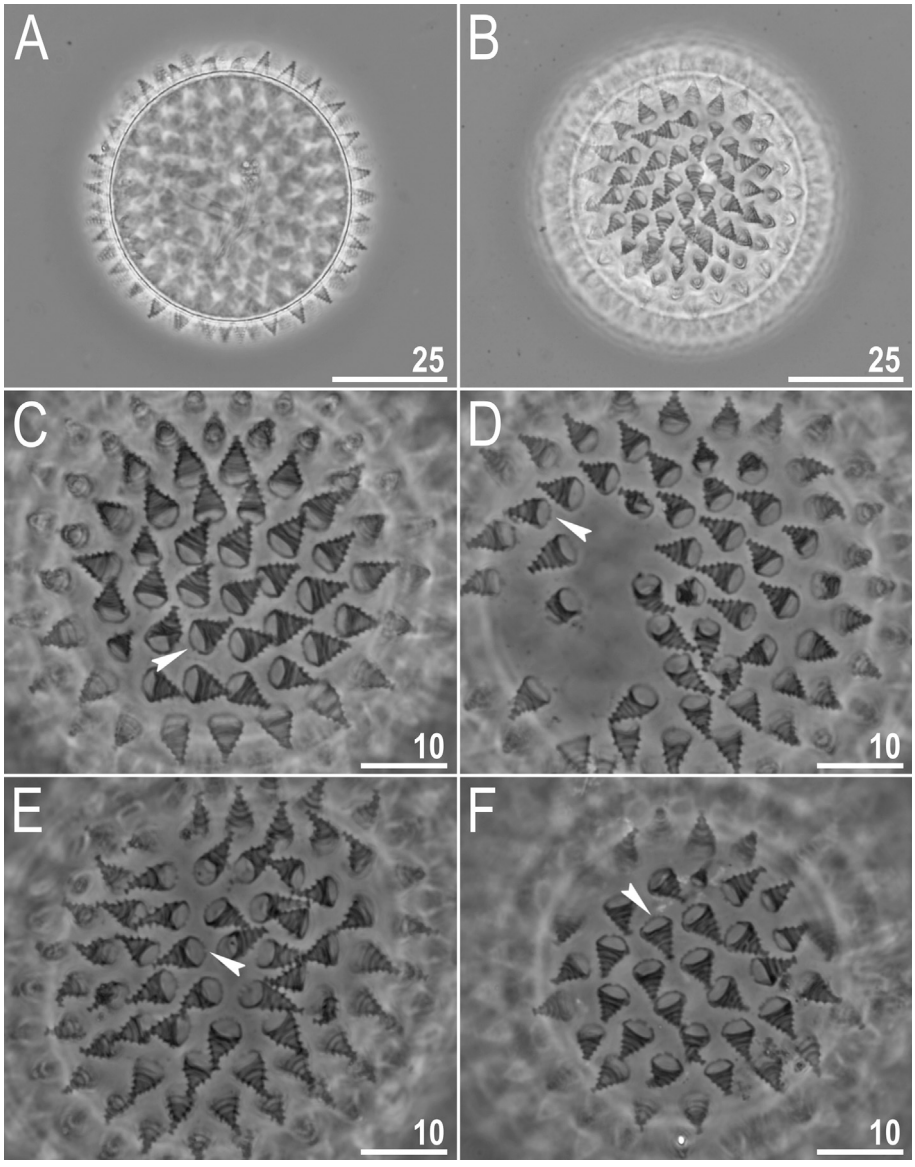

Fig. 13. ***M. pentannulatus*** **Londoño et al., 2017 from Tanzania – eggs seen in PCM. (A)** Midsection under a 400 × magnification. **(B)** Surface under a 400 × magnification. **(C–F)** Details of the egg shell under a 1000 × magnification. Filled indented arrowheads indicate faintly visible internal thickenings (attachments/sutures) at the processes bases. Scale bars in μm.

level (e.g. *Paramacrobiotus* and *Mesobiotus*; Guidetti et al., 2009; Vecchi et al., 2016; Kaczmarek et al., 2018; Guidetti et al., 2019; Guil et al., 2019; Stec et al., 2020). Importantly, the morphological hypothesis that *Minibiotus* is not monophyletic is also supported by the limited available genetic data (Guil & Giribet 2012; Bertolani et al. 2014). For example, Bertolani et al. (2014) showed that *Minibiotus furcatus* is not directly related to the few other sequenced *Minibiotus* species, but it clusters with the genus *Paramacrobiotus*. Moreover, the species exhibits spermatozoa similar to those observed in some *Paramacrobiotus* spp. and its mouth is surrounded by a ring of ten short peribuccal lamellae (instead of papulae that are supposed to be present in *Minibiotus*; but see the paragraph below). Thus, Bertolani et al. (2014) provisionally moved *M. furcatus* back to a 'basket genus' *Macrobiotus*. However, the miniaturised lamellae in *Macrobiotus furcatus* have a clearly different morphology compared to lamellae in *Macrobiotus*, *Paramacrobiotus* or *Mesobiotus*. Thus, taking into consideration both molecular phylogeny and morphology, it is likely that *M. furcatus* represents a separate genus that is yet to be described when more data are available.

The original general diagnosis of the genus has been refined in later studies (Binda & Pilato 1992; Claxton 1998; Guil & Guidetti 2005; Guidetti et al. 2007; Stec et al. 2015) and currently a species is considered as representing *Minibiotus* if its buccal apparatus conforms to the list of ten characters (see Stec et al. 2015 for the latest version of the list). The two species analysed in this study meet all these ten criteria and thus can be considered as *Minibiotus* species according to current standards. However, our study signals a potential problem with one of the key traits defining the genus, namely the peribuccal papulae. These structures are hardly visible under LCM, and SEM data for *Minibiotus* species are still extremely scarce and of varying quality (only three works comprise such SEM photographs: Schuster et al. 1980; Claxton 1998; the present study). As a result, the morphology of

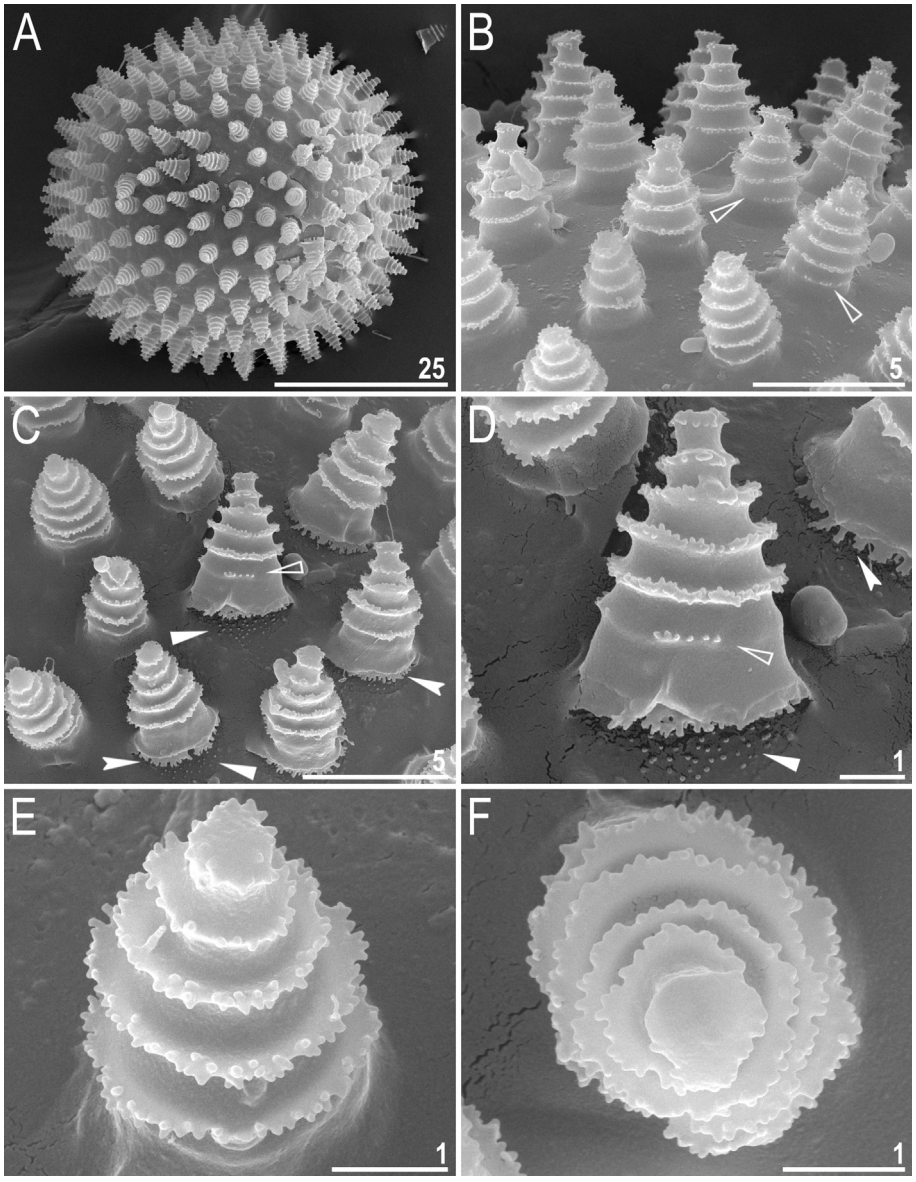

Fig. 14. ***M. pentannulatus*** **Londoño et al., 2017 from Tanzania – egg chorion seen in SEM. (A)** Entire egg. **(B–C)** Details of the egg surface. **(D–F)** Details of the processes. Empty flat arrowheads indicate undeveloped annulations, filled flat arrowheads indicate microgranulation under egg processes whereas filled indented arrowheads indicate internal thickenings (attachmants/sutures) at the processes bases. Scale bars in μm.

peribuccal papulae in *Minibiotus* has never been described in detail. With currently existing data, it is hard to determine whether peribuccal structures in *Minibiotus* should be considered as true papule (as it has been shown in Fig. 5 by Schuster et al. 1980) or rather as shortened and thickened lamellae packed closely to each other (as it has been shown in Fig. 1 by Claxton (1998) and in this study in Fig. 4C and D and 12C–D). Our photographs, being of the highest resolution among the published images, indicate that the latter scenario is more likely. However, much more effort should be made towards increasing the species sample size regarding SEM documentation of peribuccal structures in various *Minibiotus* to allow a formulation of a confident conclusion on their morphology.

Our conclusions are in line with previous studies on *Minibiotus* (Guidetti et al., 2007; Bertolani et al., 2014; Stec et al., 2015) and indicate that the genus should be considered polyphyletic. It is also obvious that this tardigrade group requires a through revision with an integrative taxonomy approach to solve the highlighted problem with the genus diagnosis as well as to test the hypothesis on putative new genera potentially hidden within the genus *Minibiotus*.

Declaration of Competing Interest

The authors declare that they have no known competing financial interests or personal relationships that could have appeared to influence the work reported in this paper.

Acknowledgments

We are especially grateful to our colleagues Bartłomiej Surmacz, Witold Morek (both of Jagiellonian University, Poland) and Thomas Pape (Natural History Museum of Denmark, University of Copenhagen) for collecting the samples which allowed us to conduct this study and to Piotr Gąsiorek who kindly extracted for us the buccal apparatuses for SEM imaging. The lichen sample containing

M. ioculator **sp. nov.** was collected from the Tradouw Pass located in Western Cape, Republic of South Africa under the permit no. CN35-28-5316 issued by CapeNature (Western Cape Province) to Witold Morek. The lichen sample containing *M. pentannulatus* was collected from the Udzungwa Mts. National Park, Tanzania under COSTECH permit No. 2015-170-ER-2012-147 to Thomas Pape and the associated TANAPA and TAWIRI permits. We also thank Rosana Londoño and Anisbeth Daza (Universidad del Magdalena, Colombia) for sending us the microphotographs of type specimens of *M. pentannulatus*. We are also grateful to two anonymous reviewers whose comments helped to improve the manuscript. The study was supported by the *Preludium* programme of the Polish National Science Centre (grant no. 2018/31/N/NZ8/03096 to DS supervised by ŁM) and by the grant from the European Commission's programme "Transnational Access to Major Research Infrastructures" to SYNTHESYS (grant no. DK-TAF-2693 to DS). Some of the analyses were carried out with the equipment purchased from the *Sonata Bis* programme of the Polish National Science Centre (grant no. 2016/22/E/NZ8/00417 to ŁM).

Appendix A. Supplementary data

Supplementary data to this article can be found online at https://doi.org/10.1016/j.jcz.2020.03.007.

References

Bertolani, R., Guidetti, R., Marchioro, T., Altiero, T., Rebecchi, L., Cesari, M., 2014. Phylogeny of Eutardigrada: new molecular data and their morphological support lead to the identification of new evolutionary lineages. Mol. Phylogenet. Evol. 76, 110–126. https://doi.org/10.1016/j.ympev.2014.03.006.

Binda, M.G., Pilato, G., 1992. *Minibiotus furcatus*, nuova posizione sistematica per *Macrobiotus furcatus* Ehrenberg, 1859, e descrizione di due nuove specie. Animalia 19, 111–120.

Binda, M.G., Pilato, G., 1995. Some notes on African tardigrades with description of two new species. Trop. Zool. 8, 367–372. https://doi.org/10.1080/03946975.1995.10539294.

Casquet, J.T., Thebaud, C., Gillespie, R.G., 2012. Chelex without boiling, a rapid and easy technique to obtain stable amplifiable DNA from small amounts of ethanol-stored spiders. Mol. Ecol. Resour. 12, 136–141. https://doi.org/10.1111/j.1755-0998.2011.03073.x.

Claxton, S.K., 1998. A revision of the genus *Minibiotus* (Tardigrada: Macrobiotidae) with descriptions of eleven new species from Australia. Record Aust. Mus. 50, 125–160. https://doi.org/10.3853/j.0067-1975.50.1998.1276.

Coughlan, K., Michalczyk, Ł., Stec, D., 2019. *Macrobiotus caelestis* sp. nov., a new tardigrade species (Macrobiotidae: *hufelandi* group) from the Tien Shan Mountains (Kyrgyzstan). Annal. Zool. 69, 499–513. https://doi.org/10.3161/00034541ANZ2019.69.3.002.

Coughlan, K., Stec, D., 2019. Two new species of the *Macrobiotus hufelandi* complex (Tardigrada: Eutardigrada: Macrobiotidae) from Australia and India, with notes on their phylogenetic position. Eur. J. Taxon. 573, 1–38. https://doi.org/10.5852/ejt.2019.573.

Da Cunha, A.X., Nascimento-Ribeiro, F., 1964. Tardigrados de Angola. Garcia Orta 12, 397–406.

Dastych, H., 1980. Niesporczaki (Tardigrada) Tatrzańskiego Parku Narodowego. Monogr. Fauny Pol. 9, 1–232.

Degma, P., Bertolani, R., Guidetti, R., 2009–2019. Actual Checklist of Tardigrada Species. https://doi.org/10.25431/11380_1178608.

Degma, P., Guidetti, R., 2007. Notes to the current checklist of Tardigrada. Zootaxa 1579, 41–53. https://doi.org/10.11646/zootaxa.1579.1.2.

Doyère, P.L.N., 1840. Memoire sur les Tardigrades. Annales des Sciences Naturelles, Series 2 (Zoologie) 14, 269–362.

Eibye-Jacobsen, J., 2001. Are the supportive structures of the tardigrade pharynx homologous throughout the entire group? J. Zool. Syst. Evol. Res. 39, 1–11. https://doi.org/10.1046/j.1439-0469.2001.00140.x.

Folmer, O., Black, M., Hoeh, W., Lutz, R., Vrijenhoek, R., 1994. DNA primers for amplification of mitochondrial cytochrome c oxidase subunit I from diverse metazoan invertebrates. Mol. Mar. Biol. Biotechnol. 3, 294–299.

Gąsiorek, G., Stec, D., Morek, W., Michalczyk, Ł., 2019. Deceptive conservatism of claws: distinct phyletic lineages concealed within Isohypsibioidea (Eutardigrada) revealed by molecular and morphological evidence. Contrib. Zool. 88, 78–132. https://doi.org/10.1163/18759866-20191350.

Gąsiorek, P., Stec, D., Morek, W., Zawierucha, K., Kaczmarek, Ł., Lachowska-Cierlik, D., Michalczyk, Ł., 2016. An integrative revision of *Mesocrista* Pilato, 1987 (Tardigrada: Eutardigrada: Hypsibiidae). J. Nat. Hist. 50, 2803–2828. https://doi.org/10.1080/00222933.2016.1234654.

Gąsiorek, P., Stec, D., Zawierucha, Z., Kristensen, R.M., Michalczyk, Ł., 2018. Revision of *Testechiniscus* Kristensen, 1987 (Heterotardigrada: Echiniscidae) refutes the polar-temperate distribution of the genus. Zootaxa 4472, 261–297. https://doi.org/10.11646/zootaxa.4472.2.3.

Guidetti, R., Bertolani, R., 2005. Tardigrade taxonomy: an updated check list of the taxa and a list of characters for their identification. Zootaxa 845, 1–46. https://doi.org/10.11646/zootaxa.845.1.1.

Guidetti, R., Bertolani, R., Degma, P., 2007. New taxonomic position of several *Macrobiotus* species (Eutardigrada: Macrobiotidae). Zootaxa 1471, 61–68. https://doi.org/10.11646/zootaxa.1471.1.6.

Guidetti, R., Cesari, M., Bertolani, R., Altiero, T., Rebecchi, L., 2019. High diversity in species, reproductive modes and distribution within the *Paramacrobiotus richtersi* complex (Eutardigrada, Macrobiotidae). Zool. Lett. 5, 1. https://doi.org/10.1186/s40851-018-0113-z.

Guidetti, R., Schill, R.O., Bertolani, R., Dandekar, T., Wolf, M., 2009. New molecular data for tardigrade phylogeny, with the erection of *Paramacrobiotus* gen. nov. J. Zool. Syst. Evol. Res. 47, 315–321. https://doi.org/10.1111/j.1439-0469.2009.00526.x.

Guil, N., Giribet, G., 2012. A comprehensive molecular phylogeny of tardigrades – adding genes and taxa to a poorly resolved phylum-level phylogeny. Cladistics 28, 21–49. https://doi.org/10.1111/j.1096-0031.2011.00364.x.

Guil, N., Guidetti, R., 2005. A new species of Tardigrada (Eutardigrada: Macrobiotidae) from Iberian Peninsula and canary Islands (Spain). Zootaxa 889, 1–11. https://doi.org/10.11646/zootaxa.889.1.1.

Guil, N., Jørgensen, A., Kristensen, R., 2019. An upgraded comprehensive multilocus phylogeny of the Tardigrada tree of life. Zool. Scripta 48, 120–137. https://doi.org/10.1111/zsc.12321.

Hall, T.A., 1999. BioEdit: a user-friendly biological sequence alignment editor and analysis program for Windows 95/98/NT. Nucleic Acids Symp. Ser. 41, 95–98.

Kaczmarek, Ł., Cytan, J., Zawierucha, K., Diduszko, D., Michalczyk, Ł., 2014. Tardigrades from Peru (South America), with descriptions of three new species of Parachela. Zootaxa 3790, 357–379. https://doi.org/10.11646/zootaxa.3790.2.5.

Kaczmarek, Ł., Michalczyk, Ł., 2017. The *Macrobiotus hufelandi* (Tardigrada) group revisited. Zootaxa 4363, 101–123. https://doi.org/10.11646/zootaxa.4363.1.4.

Kaczmarek, Ł., Zawierucha, K., Buda, J., Stec, D., Gawlak, M., Michalczyk, Ł., Roszkowska, M., 2018. An integrative redescription of the nominal taxon for the *Mesobiotus harmsworthi* group (Tardigrada: Macrobiotidae) leads to descriptions of two new *Mesobiotus* species from Arctic. PloS One 13 (10), e0204756. https://doi.org/10.1371/journal.pone.0204756.

Katoh, K., Misawa, K., Kuma, K., Miyata, T., 2002. MAFFT: a novel method for rapid multiple sequence alignment based on fast Fourier transform. Nucleic Acids Res. 30, 3059–3066. https://doi.org/10.1093/nar/gkf436.

Katoh, K., Toh, H., 2008. Recent developments in the MAFFT multiple sequence alignment program. Briefings Bioinf. 9, 286–298. https://doi.org/10.1093/bib/bbn013.

Kumar, S., Stecher, G., Tamura, K., 2016. MEGA7: molecular evolutionary genetics analysis version 7.0 for bigger datasets. Mol. Biol. Evol. 33, 1870–1874. https://doi.org/10.1093/molbev/msw054.

Londoño, R., Daza, A., Lisi, O., Quiroga, S., 2017. New species of water bear *Minibiotus pentannulatus* (Tardigrada: Macrobiotidae) from Colombia. Rev. Mex. Biodivers. 88, 807–814. https://doi.org/10.1016/j.rmb.2017.10.040.

Meyer, H.A., Hinton, J.G., 2009. The Tardigrada of southern Africa, with the description of *Minibiotus harrylewisi*, a new species from KwaZulu-Natal, South Africa (Eutardigrada: Macrobiotidae). Afr. Invertebr. 50, 255–268. https://doi.org/10.5733/afin.050.0203.

Michalczyk, Ł., Kaczmarek, Ł., 2003. A description of the new tardigrade *Macrobiotus reinhardti* (Eutardigrada, Macrobiotidae, *harmsworthi* group) with some remarks on the oral cavity armature within the genus *Macrobiotus* Schultze. Zootaxa 331, 1–24. https://doi.org/10.11646/zootaxa.331.1.1.

Michalczyk, Ł., Kaczmarek, Ł., 2013. The Tardigrada Register: a comprehensive online data repository for tardigrade taxonomy. J. Limnol. 72, 175–181. https://doi.org/10.4081/jlimnol.2013.s1.e22.

Mironov, S.V., Dabert, J., Dabert, M., 2012. A new feather mite species of the genus *Proctophyllodes* Robin, 1877 (Astigmata: Proctophyllodidae) from the Long-tailed Tit *Aegithalos caudatus* (Passeriformes: Aegithalidae): morphological description with DNA barcode data. Zootaxa 3253, 54–61. https://doi.org/10.11646/zootaxa.3253.1.2.

Morek, W., Stec, D., Gąsiorek, P., Schill, R.O., Kaczmarek, Ł., Michalczyk, Ł., 2016. An experimental test of eutardigrade preparation methods for light microscopy. Zool. J. Linn. Soc. 178, 785–793. https://doi.org/10.1111/zoj.12457.

Murray, J., 1907. Some South African Tardigrada. J. R. Micr. Soc. London. 5, 515–524. https://doi.org/10.1111/j.1365-2818.1907.tb01665.x.

Murray, J., 1913. African Tardigrada. J. R. Micr. Soc. London. 2, 136–144. https://doi.org/10.1111/j.1365-2818.1913.tb01014.x.

Nelson, D.R., Guidetti, R., Rebecchi, L., 2015. Phylum Tardgrada. Thorp and Covich's Freshwater Invertebrates. Academic Press, pp. 347–380. https://doi.org/10.1016/B978-0-12-385026-3.00017-6.

Pardi, L., 1941. Tardigrada. Miss. Biol. Sagan-Omo Roma Zool. 6, 221–232.

Pilato, G., 1981. Analisi di nuovi caratteri nello studio degli Eutardigradi. Animalia 8, 51–57.

Pilato, G., 1982. The systematics of Eutardigrada. A comment. Z. f. zool. Syst und Evolutionsforsch. 20, 271–284. https://doi.org/10.1111/j.1439-0469.1983.tb00553.x.

Pilato, G., Binda, M.G., 2010. Definition of families, subfamilies, genera and subgenera of the Eutardigrada, and keys to their identification. Zootaxa 2404, 1–52. https://doi.org/10.11646/zootaxa.2404.1.1.

Pilato, G., Claxton, S.K., 1988. Tardigrades from Australia. 1. *Macrobiotus hieronimi* and *Minibiotus macularta*, two new species of eutardigrades. Animalia 15, 83–89.

Plate, L., 1888. Beiträge zur Naturgeschichte der Tardigraden. Zool. Jahrb. (Anat.). 3, 487–550. https://doi.org/10.5962/bhl.part.1265.

Prendini, L., Weygoldt, P., Wheeler, W.C., 2005. Systematics of the *Damon variegatus* group of African whip spiders (Chelicerata: Amblypygi): evidence from behaviour, morphology and DNA. Org. Divers. Evol. 5, 203–236. https://doi.org/10.1016/j.ode.2004.12.004.

Ramazzotti, G., Maucci, W., 1983. Il phylum Tardigrada. Mem. Ist. Ital. Idrobiol. 41, 1–1012.

Richters, F., 1926. Tardigrada. In: Kükenthal, W., Krumbach, T. (Eds.), Handbuch der Zoologie, vol. 3. Walter de Gruyter & Co., Berlin & Leipzig, pp. 58–61.

Sands, C.J., McInnes, S.J., Marley, N.J., Goodall-Copestake, W., Convey, P., Linse, K., 2008. Phylum Tardigarda: an "individual" approach. Cladistics 24, 1–18. https://doi.org/10.1111/j.1096-0031.2008.00219.x.

Schuster, R.O., Nelson, D.R., Grigarick, A.A., Christenberry, D., 1980. Systematic criteria of Eutardigrada. Trans. Am. Microsc. Soc. 99, 284–303. https://doi.org/10.2307/3226004.

Stec, D., Gąsiorek, P., Morek, W., Kosztyła, P., Zawierucha, K., Michno, K., Kaczmarek, Ł., Prokop, Z.M., Michalczyk, Ł., 2016. Estimating optimal sample size for tardigrade morphometry. Zool. J. Linn. Soc. 178, 776–784. https://doi.org/10.1111/zoj.12404.

Stec, D., Kristensen, R.M., Michalczyk, Ł., 2018a. Integrative taxonomy identifies *Macrobiotus papei*, a new tardigrade species of the *Macrobiotus hufelandi* complex (Eutardigrada: Macrobiotidae) from the Udzungwa mountains National Park (Tanzania). Zootaxa 4446, 273–291. https://doi.org/10.11646/zootaxa.4446.2.7.

Stec, D., Krzywański Ł., Zawierucha, K., Michalczyk, Ł., 2020. Untangling systematics of the *Paramacrobiotus areolatus* species complex by an integrative redescription of the nominal species for the group, with multilocus phylogeny and species delineation within the genus *Paramacrobiotus*. Zool. J. Linn. Soc 188, 694–716. https://doi.org/10.1093/zoolinnean/zlz163.

Stec, D., Morek, W., Gąsiorek, P., Michalczyk, Ł., 2018b. Unmasking hidden species diversity within the *Ramazzottius oberhaeuseri* complex, with an integrative redescription of the nominal species for the family Ramazzottiidae (Tardigrada: Eutardigrada: Parachela). System. Biodiversity 16, 357–376. https://doi.org/10.1080/14772000.2018.1424267.

Stec, D., Smolak, R., Kaczmarek, Ł., Michalczyk, Ł., 2015. An integrative description of *Macrobiotus paulinae* sp. nov. (Tardigrada: Eutardigrada: Macrobiotidae: *hufelandi* group) from Kenya. Zootaxa 4052, 501–526. https://doi.org/10.11646/zootaxa.4052.5.1.

Stec, D., Zawierucha, K., Michalczyk, Ł., 2017. An integrative description of *Ramazzottius subanomalus* (Biserov, 1985) (Tardigrada) from Poland. Zootaxa 4300, 403–420. https://doi.org/10.11646/zootaxa.4300.3.4.

Teunissen, R.J.H., 1938. Tardigraden. Exploration du Parc National Albert. Mission de Witte 16, 1–21.

Thulin, G., 1928. Über die Phylogenie und das System der Tardigraden. Hereditas 11, 207–266. https://doi.org/10.1111/j.1601-5223.1928.tb02488.x.

Vecchi, M., Cesari, M., Bertolani, R., Jönsson, K.I., Rebecchi, L., Guidetti, R., 2016. Integrative systematic studies on tardigrades from Antarctica identify new genera and new species within Macrobiotoidea and Echiniscoidea. Invertebr. Systemat. 30, 303–322. https://doi.org/10.1071/IS15033.